THE ASTROPHYSICAL JOURNAL, 506:898–912, 1998 October 20

PROTOSTELLAR COSMIC RAYS AND EXTINCT RADIOACTIVITIES IN METEORITES

TYPHOON LEE
Institute of Earth Science, Academia Sinica, Taipei 115, TAIWAN
FRANK H. SHU AND HSIEN SHANG
Department of Astronomy, University of California, Berkeley, Berkeley, CA 94720-3411
ALFRED E. GLASSGOLD
Department of Physics, New York University, New York, NY 10003
AND
K. E. REHM
Argonne National Laboratory, Argonne, IL 60439-4832
Received 1998 March 24; accepted 1998 May 28

ABSTRACT

Calcium-aluminum–rich inclusions (CAIs) and chondrules of chondritic meteorites may originate with the melting of dustballs launched by a magnetically driven bipolar outflow from the inner edge of the primitive solar nebula. Bombardment by protostellar cosmic rays may make the rock precursors of CAIs and chondrules radioactive, producing radionuclides found in meteorites that are difficult to obtain with other mechanisms. Reasonable scalings from the observed hard X-rays for the cosmic-ray protons released by flares in young stellar objects yield the correct amounts of ^{41}Ca, ^{53}Mn, and ^{138}La inferred for meteorites, but proton- and α-induced transformations underproduce ^{26}Al by a factor of about 20. The missing ^{26}Al may be synthesized by ^{3}He nuclei accelerated in impulsive flares reacting primarily with ^{24}Mg, an abundant isotope in the target precursor rocks. The mechanism allows a simple explanation for the very different ratios of ^{26}Al/^{27}Al inferred for normal CAIs, CAIs with fractionated and unidentified nuclear (FUN) anomalies, and chondrules. The overproduction of ^{41}Ca by analogous ^{3}He reactions and the case of ^{60}Fe inferred for eucritic meteorites require special interpretations in this picture.

Subject headings: cosmic rays — meteors, meteoroids — nuclear reactions, nucleosynthesis, abundances — solar system: formation — Sun: particle emission

1. INTRODUCTION

Beginning with ^{129}I (Reynolds 1960; Jeffreys & Reynolds 1961), meteoriticists have surprised and puzzled workers interested in the origins of planetary systems with the discovery that many radionuclides with mean lives shorter than about 25 Myr were present 4.56×10^9 yr ago in rocky planetesimals. Table 1 lists the mean lives and relative abundances of the unambiguously determined cases (see also Swindle 1993; Wasserburg, Busso, & Gallino 1996).[1] Radionuclides with longer mean lives are less interesting since a greater number of astrophysical sources have a chance to contribute to their production (see below).

Lee, Papanastassiou, & Wasserburg (1976, 1977) found excess ^{26}Mg (hereafter denoted ^{26}Mg*) in the calcium-aluminum–rich inclusions (CAIs) of the Allende meteorite to correlate with ^{27}Al, demonstrating that ^{26}Al (the parent radionuclide of ^{26}Mg*) must have been alive at the time that aluminum was incorporated in such rocks. They concluded that either external nucleosynthetic events (novae, supernovae, etc.) seeded the pre–solar nebula cloud with ^{26}Al before the cloud went into gravitational collapse or bombardment of stable target nuclei (e.g., ^{27}Al or ^{24}Mg) by an intense flux of low-energy cosmic rays occurred in the early solar system and initiated favorable nuclear reactions.

With the accumulation of additional data, it has become clear that the distinction between the two alternatives has consequences that reach beyond the concerns of meteoriticists alone. If the external seeding hypothesis is correct in its usually stated form, the interval between the stellar production of short-lived radionuclides and their incorporation into millimeter- and centimeter-sized CAIs in the solar system occupied a few times 10^5 yr or less (see below). This suggests a fast trigger for the formation of the solar system, yet surveys of hundreds of molecular cloud cores that should give rise to sunlike stars after a wait time of a few times 10^5 yr (see, e.g., Jajina, Myers, & Adams 1998) have yet to find a single cloud core (or protostar or T Tauri star) to be enveloped within a supernova remnant or the wind cavity of an *evolved* star. Also, with a uniform seeding hypothesis, the assembly of CAIs with chondrules into planetesimals took longer than 5 Myr (see below). Since classical T Tauri stars possess dusty disks for only 1–3 Myr (see, e.g., Figs. 10*a* and 10*b* of Hartmann, Cassen, & Kenyon 1997), special circumstances again appear to be required for the origin of our own solar system. In contrast, if the internal production scenario is correct, different levels of live radionuclides inferred for different rocks do not immediately translate to intervals of time before the solidification of these rocks, and these difficulties disappear.

[1] Other frequently discussed radioactivities shorter lived than ^{129}I are ^{135}Cs and ^{182}Hf, which have mean lives of 3.3 and 13 Myr, respectively. The initial abundances for ^{135}Cs/^{133}Cs and ^{182}Hf/^{180}Hf have been inferred by McCulloch & Wasserburg (1978) and by Lee & Halliday (1995) to be 2×10^{-4} and 3×10^{-4}, respectively. These inferences are based, however, on deficits of ^{135}Ba and ^{182}W seen in calcium-aluminum–rich inclusions (CAIs) and iron meteorites, respectively, and thus do not give unequivocal evidence for live ^{135}Cs or ^{182}Hf in the early solar system. In fact, the ^{135}Ba deficit has been alternatively interpreted by its discoverers as the result of unusual *s*-process nucleosynthesis. Birck & Lugmair (1988) have set an upper limit of ^{60}Fe/^{56}Fe $= 1.6 \times 10^{-6}$ for Allende CAIs. Excesses of ^{60}Ni relative to ^{58}Ni are seen, not excesses of ^{60}Ni, which correlates with ^{56}Fe; therefore, the identification with ^{60}Fe decay is ambiguous. Indeed, if ^{58}Ni and ^{61}Ni are assumed to be normal, ^{60}Ni, ^{62}Ni, and ^{64}Ni are anomalous. Without much actual ^{60}Fe production, the nickel anomalies may arise from unusual stellar processing or by cosmic-ray bombardment of stable nickel isotopes and their immediate neighbors in the periodic table.

TABLE 1

EXTINCT RADIONUCLIDES

Ratio	Mean Life (Myr)	Relative Abundance	Reference
$^{41}Ca/^{40}Ca$	0.15	1.5×10^{-8}	Srinivasan et al. 1994
$^{26}Al/^{27}Al$	1.1	5×10^{-5}	Lee et al.1976
$^{60}Fe/^{56}Fe$.....	2.2	4×10^{-9}	Shukolykov & Lugmair 1993a
$^{53}Mn/^{55}Mn$	5.3	4×10^{-5}	Birck & Allégre 1985
$^{107}Pd/^{108}Pd$.....	9.4	2×10^{-5}	Kelly & Wasserburg 1978
$^{129}I/^{127}I$	23	1×10^{-4}	Jeffreys & Reynolds 1961

The single entries in the third column of Table 1 do not imply that unique values for the abundance ratio of radionuclides to stable isotopes apply to all meteoritic material. The problem has been studied thoroughly for $^{26}Al/^{27}Al$, for which an important result holds (MacPherson, Davis, & Zinner 1995). In the normal CAIs of carbonaceous chondrites the distribution is distinctly bimodal, with a large peak at $^{26}Al/^{27}Al = 4.5 \times 10^{-5}$ and a sharp upper cutoff at $\sim 5.5 \times 10^{-5}$, and a smaller peak at $^{26}Al/^{27}Al = 0$ with another upper cutoff near $^{26}Al/^{27}Al = 9 \times 10^{-6}$ (see Fig. 1). The smaller peak at 0 may be due to postsolidification equilibration between Mg-rich and Mg-poor phases (Podosek et al. 1991; MacPherson & Davis 1993; Caillet, MacPherson, & Zinner 1993). However, this explanation cannot apply to those minority CAIs possessing fractionated and unidentified nuclear (FUN) and unidentified nuclear (UN) isotopic anomalies, in which the $^{26}Al/^{27}Al$ distribution shows a single peak at $^{26}Al/^{27}Al = 0$ with an upper cutoff again near 9×10^{-6} (Lee et al. 1976; Clayton & Mayeda 1977; Wasserburg, Lee, & Papanastassiou 1977; Ireland et al. 1992). The anomalies of stable isotopes found in the FUN inclusions suggest that these CAIs have the best retained memory of their original nucleosynthetic sources, yet they do not show the canonical abundance ratio of 5×10^{-5}.

A similar pattern seems to hold for ordinary chondrites, although the data here are understandably more sparse since their CAIs are rarer and smaller than those in carbonaceous chondrites. In particular, the CAIs in the ordinary chondrite Chainpur have $^{26}Al/^{27}Al$ ratios $\sim 5 \times 10^{-5}$ (Russell et al. 1996). In the same meteorite, two Al-rich chondrules have an inferred ratio of $\sim 9 \times 10^{-6}$, whereas five other Al-rich chondrules have no resolvable $^{26}Mg^*$ resulting from ^{26}Al decay. If all solar system material started with the same ratio of $^{26}Al/^{27}Al = 5 \times 10^{-5}$, some chondrules must have solidified 5 Myr later than the CAIs with which they are later found to be more or less uniformly distributed within centimeters of each other.

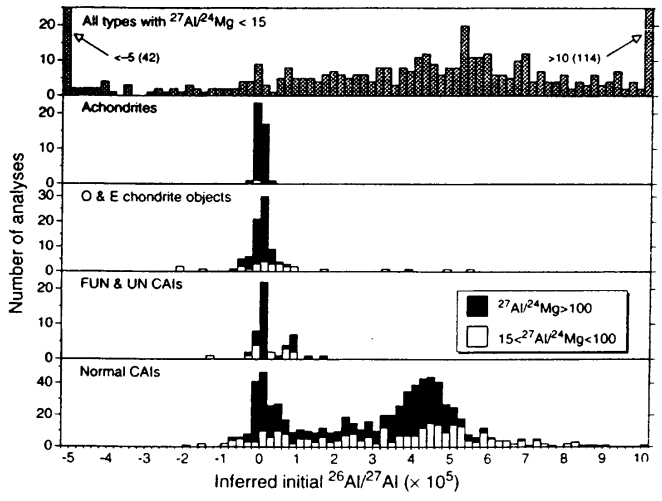

FIG. 1.—Histogram of the distribution of $^{26}Al/^{27}Al$ in achondrites, the chondrules of ordinary and enstatite chondrites, FUN and UN CAIs, and normal CAIs. Measurements in aluminum-rich samples where $^{27}Al/^{24}Mg > 100$ are more reliable than measurements in samples where $^{27}Al/^{24}Mg < 100$ and, even more so, than in those where $^{27}Al/^{24}Mg < 15$. (Reprinted with permission from MacPherson et al. 1995.)

CAIs and chondrules are objects that have experienced intense but brief heating events in the early solar system (see, e.g., Shu et al. 1997; Shu, Shang, & Lee 1996). In this paper we will argue that they also underwent related nuclear processing. In contrast, individual presolar grains found in chondritic meteorites of corundum (Al_2O_3), graphite, and silicon carbide—probably condensation ejecta from supernovae and carbon stars that did not melt and had their constituents mix with other materials in the solar nebula (Clayton 1975)—show a wide variation in abundance of $^{26}Mg^*/^{27}Al$, ranging from less than 1×10^{-5} to nearly 1 (see Fig. 14 of MacPherson et al. 1995). As demonstrated by analysis of the exposure time of these grains to Galactic cosmic rays (Anders & Zinner 1993), most of the ^{26}Al once in these grains did not come into the solar system alive.

Clayton & Leising have computed the average interstellar value of various radioactivities expected by stellar nucleosynthesis and reasonable models of molecular cloud mixing (Clayton 1983; Clayton & Leising 1984). They showed that ^{129}I and ^{107}Pd should be roughly 10 times as abundant in average clouds as they are inferred to be in the primitive solar nebula (Jeffreys & Reynolds 1961; Kelly & Wasserburg 1978); thus, these radionuclides require neither a late nucleosynthetic injection event nor production within the early solar system. The case of ^{53}Mn is ambiguous, and Clayton & Leising calculated ^{26}Al to exist at average values too small to account for either the observed meteoritic ratios or the low level that it is actually detected in the interstellar medium through the emission of gamma-ray lines at 1.809 MeV (Mahoney et al. 1984; Diehl et al. 1994, 1995).

Most workers adopt the hypothesis that the birth of the solar system occurred in a molecular cloud core that was seeded by nearby stellar nucleosynthetic events in many of the short-lived radioactivities (but perhaps not ^{129}I and ^{107}Pd) at the indicated levels of Table 1 (Wasserburg 1985; Cameron 1995). However, the need to get enough live ^{41}Ca from its stellar creation site into solidified CAIs sets tight time constraints that are difficult to reconcile with theories and observations of the formation of sunlike stars (Shu, Adams, & Lizano 1987; Cameron 1988). For example, if a

supernova provides both the meteoritic ^{26}Al and ^{41}Ca, Srinivasan et al. (1996) estimate a self-consistent free-decay time of 1.5 Myr. However, an abundance of live ^{41}Ca after such an interval that equals 1.5×10^{-8} of *all* ^{40}Ca (Srinivasan, Ulyanov, & Goswami 1994) would then be accompanied by a decay counterpart, assuming the same injection probability of live and dead nuclides, that would equal the *entire* ^{41}K content of the solar system (namely, $^{41}\mathrm{K}/^{40}\mathrm{Ca} = 4 \times 10^{-3}$). Srinivasan et al. (1996) reject as unrealistic the possibility that a single injection event could be responsible for a good fraction of the stable K, Ca, Mg, and Al in the solar system. Thus, if a late nucleosynthetic event really did take place, free-decay times much shorter than 1.5 Myr should be contemplated. Unfortunately, contributions from a late supernova (Harper 1996) may still have to be combined with those from a rare asymptotic giant branch (AGB) star whose distance from the solar system 4.56×10^9 yr ago was closer than that of Proxima Centauri today (Cameron 1993; Wasserburg et al. 1994; Kastner & Myers 1994). The problem is that supernovae cannot make enough ^{26}Al (Cameron et al. 1995), while AGB stars cannot make any ^{53}Mn (Wasserburg et al. 1994).

In this paper, we shall explore the possibility that the most obstinate short-lived radionuclides, ^{26}Al, ^{41}Ca, and ^{53}Mn, were actually made by cosmic-ray bombardment in the early solar system (Fowler et al. 1962; Clayton, Dwek, & Woosley 1977; Dwek 1978; Lee 1978; Feigelson 1982; Clayton & Jin 1995a). An alternative scenario, spallation reactions in the interstellar medium by Galactic cosmic rays, is discussed in Appendix A. The case of ^{60}Fe is complex and is discussed in § 6 and Appendix B.

2. THE UNDERLYING ASTROPHYSICAL MODEL

We adopt the fluctuating x-wind picture for producing CAIs and chondrules as our underlying irradiation model (Shu et al. 1997). In this picture (see Fig. 2), long-term fluctuations, associated perhaps with magnetic cycles with timescales $\Delta t \sim$ decades, are superimposed on top of a time-averaged flow in which disk accretion at a rate $\dot{M}_D$ divides at the inner disk radius R_x into a funnel flow onto a star with an accretion rate $\dot{M}_* = (1 - f)\dot{M}_D$ and an x-wind with

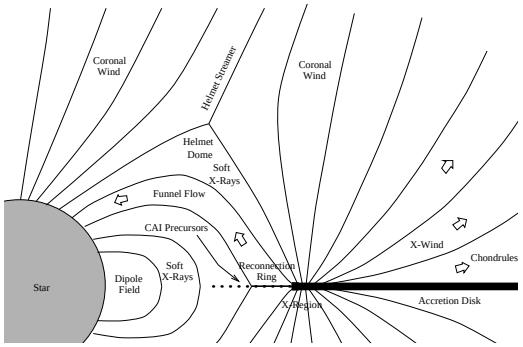

FIG. 2.—Schematic drawing of the magnetic field geometry and gas flow in the x-wind model for the production of CAIs and chondrules. While chondrules are being launched from the x-region, cosmic-ray irradiation of CAI precursors occurs by impulsive flares in the reconnection ring, where the distorted dipole field makes an excursion to the x-region as a part of the magnetic flux trapped there. The figure indicates that thermally driven coronal winds from the star and the disk may help the magnetocentrifugally driven x-wind to open field lines surrounding the helmet streamer, but this aspect of the configuration is not essential to our model. (Reprinted from Shu et al. 1997.)

an outflow rate $\dot{M}_w = f\dot{M}_D$. On dimensional grounds, R_x is given by the scaling of Ghosh & Lamb (1978):

$$R_x = \Phi_{dx}^{-4/7}\left(\frac{\mu_*^4}{GM_*\dot{M}_D^2}\right)^{1/7}, \tag{1}$$

where G is the universal gravitation constant and M_* and μ_* are, respectively, the mass and dipole magnetic moment of the star. For our "preferred model" (Najita & Shu 1994; Ostriker & Shu 1995), $f \approx \frac{1}{3}$ and $\Phi_{dx} = 1.15$. As a long-term average, the rotation rate of the star, Ω_*, is mechanically locked to the Keplerian angular speed of the inner edge of the disk (cf. Königl 1991; Edwards et al. 1993),

$$\Omega_x = \left(\frac{GM_*}{R_x^3}\right)^{1/2}, \tag{2}$$

but fluctuations in μ_* or $\dot{M}_D$, combined with the relatively quick response of the disk and the large inertia of the star, lead to instantaneous conditions under which $\Omega_* \neq \Omega_x$. We may expect the resulting shear of magnetic field lines connected to both the accretion disk and the star to build up excess field energy. The sporadic release of the energy stored in the stressed fields generates fast flare particles and hard X-rays. Gradual flares and coronal mass ejections (CMEs) yield fast protons and α-particles by shockwave acceleration, whereas reconnection events preceding or following CMEs produce a large excess of fast ^{3}He particles, probably by resonant wave-particle acceleration. The latter is similar to processes that operate in impulsive flares in the present solar corona (Cliver 1996).

The geometry of trapped stellar flux in the x-region produces a configuration just interior to R_x, denoted by the label "reconnection ring" in Figure 2, which has reversed poloidal magnetic fields across the midplane (Ostriker & Shu 1995). Field reversals naturally create an environment conducive to fast reconnection events and magnetic flares. Rocks that fall into the reconnection ring from the funnel flow (or that drift into it from the gaseous disk) will be exposed to irradiation by the fast particles accelerated in gradual and impulsive flares. Thus, the reconnection ring constitutes a powerful irradiation zone for the production of short-lived radioactivities in protosolar rocks. Rocks irradiated in the reconnection ring during a period when R_x is relatively large (because μ_* is strong or $\dot{M}_D$ is weak) can later be picked up and launched in the x-wind when a fluctuation (a decrease in μ_* or an increase in $\dot{M}_D$) causes the base of the x-wind R_x to migrate to the region previously occupied by such rocks. Provided the irradiated, heated, and melted rocks have an appropriate range of sizes, they can then be flung to planetary distances, where they are incorporated as CAIs and chondrules in growing planetesimals (see Tables 1 and 2 of Shu et al. 1997 for numerical examples).

When $\Omega_* \neq \Omega_x$, field lines connected to both the star and the x-region will wrap up, increasing the magnetic energy of the configuration at a rate (cf. eq. [1] of Shu et al. 1997)

$$\frac{dE_{\mathrm{mag}}}{dt} = \eta\,|\Omega_* - \Omega_x|\,\frac{\mu_*^2}{R_x^3}, \tag{3}$$

where η is a dimensionless form factor that depends on the specifics of the field geometry. We suppose that $|\Omega_* - \Omega_x|$ is typically some fraction S of Ω_x and that another fraction $\epsilon_p^m(E_p)$ of the magnetic energy release goes to accelerating

fast protons with energy $E \geq E_p$. If we now eliminate μ_* and Ω_x by using equations (1) and (2), we get, for the time-averaged luminosity L_p of protons with $E \geq E_p$,

$$L_p(E \geq E_p) = \epsilon_p^g(E_p) \frac{GM_* \dot{M}_D}{R_x} ,$$

where

$$\epsilon_p^g(E_p) \equiv \eta \Phi_{dx}^2 S \epsilon_p^m(E_p) \quad (4)$$

is the time-averaged efficiency for accelerating such protons, measured in units of the basic scale of gravitational energy release by the disk accretion at its inner edge. If we likewise define $\epsilon_x^m(E_x)$ as the time-averaged fraction of the magnetic energy release in flares that goes into X-rays of energy $E \geq E_x$, we obtain

$$L_x(E \geq E_x) = \epsilon_p^g(E_x) \frac{GM_* \dot{M}_D}{R_x} ,$$

where

$$\epsilon_x^g(E_x) \equiv \eta \Phi_{dx}^2 S \epsilon_x^m(E_x) . \quad (5)$$

Dividing equation (4) by equation (5), we get

$$\frac{L_p(E \geq E_p)}{L_x(E \geq E_x)} = \frac{\epsilon_p^g(E_p)}{\epsilon_x^g(E_x)} = \frac{\epsilon_p^m(E_p)}{\epsilon_x^m(E_x)} . \quad (6)$$

In principle, the last ratio of magnetic efficiencies $\epsilon_p^m/\epsilon_x^m$ is obtainable by comparing the gamma rays produced by energetic ions to the X-rays released in flares on the modern sun. On the other hand, the denominator $L_x(E \geq E_x)$ in the first ratio is measurable from satellite X-ray observations of young stellar objects (YSOs). The combination yields a method by which we can obtain estimates of $L_p(E \geq E_p)$ or, equivalently, $\epsilon_p^g(E_p)$, in YSOs.

In the case of impulsive flares, the production of protons with $E \geq E_{10} \equiv 10$ MeV over solar cycle 21 (peak in 1980) lasting $\Delta t = 11$ yr corresponds to $L_p^{\rm imp}(E \geq E_{10})\Delta t = 4 \times 10^{31}$ ergs (Ramaty & Simnett 1991). Over such a cycle, there are approximately 2600 M-class flares, each releasing an estimated energy in hard X-rays of $\sim 10^{29}$ ergs, and 170 X-class flares, each releasing an estimated energy in hard X-rays $\sim 10^{30}$ ergs. This gives a total $L_x^{\rm hard}\Delta t = 4.3 \times 10^{32}$ ergs in X-rays between about 1.6 and 12 keV (Haisch, Antunes, & Schmitt 1995), implying a mean ratio $L_p^{\rm imp}(E \geq E_{10}) = 0.09 L_x^{\rm hard}$ that we adopt also as applying to YSOs.

The luminosities $L_x^{\rm hard}$ in hard (0.4–12 keV) X-rays for five embedded protostellar sources in the nearby dark cloud R CrA range over $2–12 \times 10^{30}$ ergs s^{-1}, with a mean of 4×10^{30} ergs s^{-1}; they range over $5–10 \times 10^{30}$ ergs s^{-1} for three such sources in the Rho Oph cloud, with a mean of 8×10^{30} ergs s^{-1} (Koyama et al. 1996; Neuhäuser & Preibisch 1997; Preibisch 1997; Kamata et al. 1997). We adopt as a representative value $L_x^{\rm hard} = 5 \times 10^{30}$ ergs s^{-1}, yielding $L_p^{\rm imp}(E \geq E_{10}) = 0.09 L_x^{\rm hard} = 4 \times 10^{29}$ ergs s^{-1}. The bolometric luminosity of sunlike YSOs, a few $L_\odot$, comes largely from accretion and is therefore comparable to $GM_* \dot{M}_D/R_*$ (Shu et al. 1987). In typical x-wind models, R_x is a few times R_*. Thus, as a time average, the scale factor $GM_* \dot{M}_D/R_x$ for a typical YSO might be 1 $L_\odot$ or 4×10^{33} ergs s^{-1}. With these numbers, equation (4) now implies

$$\epsilon_p^g(E_{10}) \equiv \epsilon_{10} = 1 \times 10^{-4} \quad (7)$$

for impulsive flares in sunlike YSOs. As we shall see, this rough estimate is remarkably similar to the value needed to understand extinct radioactivities in meteorites.

The hour-by-hour variation by factors of 2 and larger of hard X-ray flux from young and old T Tauri stars (see Fig. 8 of Carkner et al. 1996) suggests that most of observed activity in YSOs is associated with large and small impulsive flares. It is considerably more difficult to try to estimate the particle production by gradual flares, since CMEs produce copious protons but few electrons, and therefore little X-ray emission (Gosling 1993; Reames 1995). Moreover, what flare electrons are generated travel predominantly outward and escape to space rather than produce radiation by bremsstrahlung when they strike the surface of the star. In the case of the modern sun, artificial satellites can directly detect the outwardly propagating ions on open field lines from gradual flares more readily than they can detect energetic ions accelerated on closed field lines from impulsive flares that erupt close to the solar surface. A bias arises therefore that gradual flares contribute more to the cosmic-ray bombardment of solar-system rocks than impulsive flares. This perception may be false if the rocks lie within a few stellar radii of the protosun. To simplify the discussion below, we shall invoke primarily impulsive flares, for which we have a reasonable if rough scaling method via equation (7), and appeal to gradual flares only for the bombardment of rocks at planetary distances (e.g., see § 6).

3. NUCLEOSYNTHESIS BY CHARGED PARTICLES IN THE RECONNECTION-RING MODEL

Fast charged particles generated by CMEs (gradual flares) or magnetic reconnection (impulsive flares) involving the helmet streamer in Figure 2 either travel outward along field lines that open to interstellar space or fly inward along field lines that have footpoints in the star or the x-region of the disk. Per cosmic ray, irradiation of the x-region is very inefficient in producing radionuclides because most of the fast particles are stopped by interactions with gas atoms (Fowler et al. 1962). We ignore this process in the remaining discussion and concentrate on the flares that occur in the reconnection ring.

The gas disk is truncated within $\sim 0.03 R_x$ of R_x (Najita & Shu 1994; Ostriker & Shu 1995); thus, most of the reconnection ring below the funnel flow from $0.75 R_x$ to R_x is occupied by coronal plasma. From soft X-ray observations of young stellar objects, we deduce that the coronal plasma in the neighborhood of the reconnection ring has a radial column density $\rho_g \Delta R \sim 10^{-4}$ g cm^{-2} (Shu et al. 1997). Such a small column has little effect on MeV cosmic-ray ions. Instead, the latter are entirely spent by their interactions with rocks in this region. The ability to irradiate essentially bare rock in the same general region (reconnection ring) where the cosmic rays are generated represents a considerable advantage (amounting to a few orders of magnitude) of our scheme relative to earlier ones (Fowler et al. 1962).

Let $m_r \sim 25$ amu be the typical mass of an atom in the precursor rock. Then the number of atoms of a stable isotope S (e.g., ^{27}Al) passing through the irradiation zone equals

$$N_S = x_S^r F X_r \dot{M}_D \Delta t / m_r , \quad (8)$$

where x_S^r is the number fraction of S atoms in rock r. In equation (8), $X_r \dot{M}_D \Delta t$ is the mass of refractory rock of cosmic mass fraction $X_r = 4 \times 10^{-3}$ carried by disk accre-

tion into the x-region and beyond in time Δt. Of this rock mass, we assume a fraction F either falls out of the funnel flow or is too big to be lifted by either the x-wind or the funnel flow and drifts past the inner edge of the disk to enter the irradiation zone of the reconnection ring.

A calculation from first principles of F would require knowledge of the size distribution of dustballs that enter the x-region by accretion from the external disk. Lacking this knowledge, we adopt a numerical choice $F \sim 0.01$ consistent with processing *all* the rock that ends up in the planets of the solar system as CAIs or chondrules experiencing some irradiation in the reconnection ring. (We assume that rocks appropriately sized to drop out of the funnel flow when a fluctuation makes R_x larger [smaller $\dot{M}_D$ or larger μ_*] is also appropriately sized to drop out of the x-wind flow when a fluctuation makes R_x smaller [larger $\dot{M}_D$ or smaller μ_*].) The choice $F = 0.01$ is apt if the funnel flow itself [carrying $\sim(2/3)\dot{M}_D$] supplies the 1 $M_\odot$ that goes into making the mass of the sun, and the rocky component of the planets in the solar system is that associated with 0.013 $M_\odot$ of gas (Hayashi, Nakazawa, & Nakagawa 1985). If some of the rocks that go into making planets never drifted to the inner disk edge, or were launched by the x-wind without entering the reconnection ring, F could be smaller than 0.01. For example, if no chondrules at all were irradiated, only CAIs, F could be smaller than 0.01 by a factor of 20. This extreme is not a viable choice given the discussion of § 1. Thus, we assume that irradiated rocks included magnesium-iron silicates along with calcium-aluminum oxides and silicates, but that only CAI-like material survived subsequent heating in the x-wind if this material traversed deep enough into the reconnection ring to receive a full dosage of particle bombardment (see Shu et al. 1996, 1997). Chondrules can then have survived the heating in the x-wind only if their precursor rocks either never entered the reconnection ring or penetrated it only shallowly and received only a partial dosage.

The rate $\dot{N}_R$ of producing radionuclide R (e.g., ^{26}Al) through bombardment of target atoms T in rocks with space density ρ_r by cosmic rays of type CR equals

$$\dot{N}_R = V \int_{E_0}^{\infty} x_T^r \frac{\rho_r}{m_r} v f_{\rm CR}(E)\sigma(E) dE \,, \tag{9}$$

where multiplication by the volume V of the irradiation zone assumes for simplicity uniform conditions within V. In equation (9), $f_{\rm CR}(E)dE$ is the number density of CRs with energy per nucleon between E and $E + dE$, v is the CR speed, $\sigma(E)$ and E_0 are the energy-dependent cross section and threshold for the reaction $T + {\rm CR} \rightarrow R$, and x_T^r is the number fraction of target atoms T in the rock. We ignore modifications of the cosmic-ray injection spectrum due to nuclear reactions, which are small compared to the rate of energy loss $\dot{E}$ associated with Coulomb and ionization losses by passage through the rock in the reconnection ring. We may then obtain the steady state distribution function $f_{\rm CR}(E)$ impinging on the rock atoms from the kinetic equation,

$$\frac{\partial}{\partial E}\left(\dot{E} f_{\rm CR}\right) = j_{\rm CR}(E) \,, \tag{10}$$

where $j_{\rm CR}(E)dE$ is the time-averaged volumetric rate of accelerating CRs of energy per nucleon between E and $E + dE$ by flares in the reconnection ring. Writing $\dot{E} = -v\langle dE/d\ell\rangle(E)$, where $\langle dE/d\ell\rangle(E)$ is the absolute value of the energy-dependent loss of energy per unit length of traversal through the uniformly distributed rock material, we obtain, upon integration of equation (10) over energy per nucleon from E to ∞ and multiplication by V,

$$V v f_{\rm CR}\left\langle \frac{dE}{d\ell} \right\rangle (E) = V \int_E^{\infty} j_{\rm CR}(E')dE' \equiv \dot{N}_{\rm CR}(E) \,, \tag{11}$$

where $\dot{N}_{\rm CR}(E)$ is the time-averaged rate of production of CRs with energy per nucleon greater than E in the entire reconnection ring. For simplicity, we assume that the differential distribution $d\dot{N}_{\rm CR}/dE$ has the same power-law spectra as solar energetic particles (SEPs): $d\dot{N}_{\rm CR}/dE \propto E^{-p}$, where $p \approx 2.7$ for gradual flares (Van Hollenbeke, Sung, & McDonald 1975) and $p \approx 3.5$ for impulsive flares when $E >$ 1 MeV amu^{-1} (Temerin & Roth 1992; Reames et al. 1997). The relationship between $\dot{N}_p$ and the luminosity L_p of protons with $E \geq E_p$ then equals

$$\dot{N}_p = \frac{(p-2)L_p}{(p-1)E_p} \propto E_p^{-(p-1)} \,. \tag{12}$$

The substitution of equation (11) into equation (9) yields

$$\dot{N}_R = \int_{E_0}^{\infty} \frac{x_T^r \rho_r \dot{N}_{\rm CR}(E)\sigma(E)dE}{m_r \langle dE/d\ell\rangle(E)} \,. \tag{13}$$

Despite the somewhat unusual circumstances of the derivation, this equation is the usual "thick target" formula for cosmic-ray nucleosynthesis (see eq. [1] of Ramaty, Kozlovsky, & Lingenfelter 1996, in which we reverse the order of the two integrations). In the energy range of interest, we may approximate $\langle dE/d\ell\rangle \propto E^{-q}$ with $q \approx 0.7$ (Reedy & Marti 1991; Clayton & Jin 1995a). Writing $\langle dE/d\ell\rangle(E) = \langle dE/d\ell\rangle(E_0)(E/E_0)^{-q}$ and beginning with $\ell = 0$ when $E = E_0$, we may compute for later reference the stopping length $\ell_0(E_0)$ when $E = 0$ as

$$\ell_0(E_0) = \frac{E_0}{(q+1)\langle dE/d\ell\rangle(E_0)} \,. \tag{14}$$

Similarly, writing $\dot{N}_{\rm CR}(E) = \dot{N}_{\rm CR}(E_0)(E/E_0)^{-(p-1)}$ allows us to evaluate the rate of production of R as

$$\dot{N}_R = \eta_{\rm TR}^r \dot{N}_{\rm CR}(E_0) \,,$$

with

$$\eta_{\rm TR}^r = (q+1)x_T^r \mathscr{A} \Sigma_{\rm CR}^r \sigma_0 / m_r \,, \tag{15}$$

where $\Sigma_{\rm CR}^r(E_0)$ is the stopping column for cosmic rays of energy per nucleon E_0 in rock,

$$\Sigma_{\rm CR}^r(E_0) \equiv \rho_r \ell_0(E_0) \,, \tag{16}$$

$\sigma_0 \equiv 10^{-25}$ cm^2 is a fiducial nuclear cross section (100 mbarn), and $\mathscr{A}$ is a dimensionless form factor characterizing a weighted height and width of the cross section $\sigma(E)$:

$$\mathscr{A} \equiv \int_{E_0}^{\infty} \frac{\sigma(E)}{\sigma_0} \left(\frac{E}{E_0}\right)^{2+q-p} \frac{dE}{E} \,. \tag{17}$$

Equation (15) gives $\eta_{\rm TR}^r \ll 1$ as the nuclear yield of R from T per cosmic-ray particle of type CR bombarding rock r. In time Δt, the total number of R atoms induced by the bombardment of cosmic rays of type CR on T is

$$N_R = \eta_{\rm TR}^r \dot{N}_{\rm CR} \Delta t = (q+1)x_T^r \left(\frac{A}{Z^2}\right)_{\rm CR} \Sigma_p^r \mathscr{A} \sigma_0 y_{\rm CR} \dot{N}_p \frac{\Delta t}{m_r} \,. \tag{18}$$

In equation (18), $\dot{N}_{\rm CR}(E_0) \equiv y_{\rm CR}\,\dot{N}_p(E_p)$, with $y_{\rm CR}$ being the number fraction of species CR relative to protons at the same energy per nucleon, $E_p = E_0$, and we have assumed that $\Sigma^r_{\rm CR}(E_0)$ for a cosmic ray of charge Z and atomic weight A equals A/Z^2 times the stopping column $\Sigma^r_p(E_p)$ of a proton in rock.

Dividing equation (18) by equation (8) and using equations (12) and (4) to eliminate $\dot{N}_p$, we get

$$\frac{N_R}{N_S} = \mathscr{A}\, y_{\rm CR}\, \frac{(q+1)(p-2)}{(p-1)} \left(\frac{x^r_T}{x^r_S}\right)\left(\frac{A}{Z^2}\right)_{\rm CR} \times \left[\frac{\Sigma^r_p(E_p)\sigma_0\,\epsilon^g_p(E_p) G M_*}{F X_r R_x E_p}\right]. \tag{19}$$

Note that the combination that matters for our irradiation model is ϵ^g_p/F and that m_r, Δt, and $\dot{M}_D$ have disappeared from the calculation. The fractional radioactivity induced, N_R/N_S, does not depend on the "average" mass m_r of a rock atom when we ratio the numbers of two species. More significantly, the result does not depend on the time rocks spend in the reconnection ring, Δt, because increasing Δt increases the amount of rock brought into the reconnection ring that needs to be irradiated, but it also increases the total radiation dosage proportionally; in a thick-target situation where all cosmic rays are ultimately stopped by rock, the dosage per rock remains the same. Most significantly, N_R/N_S does not depend on the disk accretion rate $\dot{M}_D$ (i.e., in what phase of protostellar evolution the system exists), because the rate with which the disk brings rock into the reconnection ring to be irradiated and the rate with which irradiating cosmic rays are generated by the interaction of the accretion disk with the stellar magnetosphere are both proportional to $\dot{M}_D$ in our model. Thus, equation (19) yields the same relative abundance N_R/N_S for the CAIs of carbonaceous chondrites and ordinary chondrites as long as the ratio M_*/R_x remains relatively constant at different stages of the evolution of young stars.

Since $\Sigma^r_p(E_p) \propto E_p^{q+1}$ and $\dot{N}_p(E_p) \propto E_p^{-(p-1)}$ [implying $\epsilon^g_p(E_p) \propto E_p^{-(p-2)}$], the terms in the brackets of equation (19) depend on E_p as $E_p^{(2+q-p)}$. At a proton energy of $E_{10} = 10$ MeV, $\Sigma^r_p(E_{10}) = 0.2$ g cm^{-2} (Reedy & Marti 1991), and $\epsilon^g_p(E_{10}) = \epsilon_{10}$. With $\sigma_0 = 10^{-25}$ cm^2, $X_r = 4 \times 10^{-3}$, $F = 0.01$, $M_*/R_x \approx 1.3 \times 10^{21}$ g cm^{-1} during both the embedded and revealed stages of YSO evolution (Shu et al. 1996; see also Tables 1 and 2 of Shu et al. 1997), equation (19) above becomes

$$\frac{N_R}{N_S} = 2.7 \times 10^{-3}\mathscr{B}\epsilon_{10}\, y_{\rm CR}\, \frac{(q+1)(p-2)}{(p-1)} \left(\frac{x^r_T}{x^r_S}\right)\left(\frac{A}{Z^2}\right)_{\rm CR}, \tag{20}$$

where $\mathscr{B} \equiv \mathscr{A}(E_0/E_{10})^{(2+q-p)}$:

$$\mathscr{B} = \int_{E_0}^{\infty} \frac{\sigma(E)}{\sigma_0} \left(\frac{E}{E_{10}}\right)^{2+q-p} \frac{dE}{E}. \tag{21}$$

In the discussion that follows, we shall consider only charged particle reactions and ignore neutron captures initiated by secondary neutrons released, say, by (p, n) reactions. At first sight, this neglect appears unjustified since (p, n) reactions on any material (including rock) are among the most probable of any set of proton reactions, and the neutrons so generated also have large cross sections ($\sim$1 barn) for absorption and scattering. Thus, if the target is "thick," one might conclude that a large fraction of primary proton reactions would induce secondary neutron absorptions. In fact, this naive conclusion is false because a target that is thick with respect to (p, n) reactions will not necessarily be thick with respect to neutron captures.

The rocks in the reconnection ring provide a thick target for proton irradiation because of two effects. (1) The stopping column of 10 MeV protons in rock is only 0.2 g cm^{-2}, which is comparable to the column presented by individual CAIs or chondrules. (2) The magnetic field geometry in Figure 2 on either side of the reconnection ring diverts any charged particles that try to escape from the region back toward the midplane. Thus, fast protons have to traverse many times through the reconnection ring along its longest (horizontal) dimensions. This implies that they all get stopped eventually by the rocks that orbit in the midplane because of the angular momentum vector associated with the rocks having come out of a surrounding accretion disk whose inner edge acts as one footpoint for the stellar magnetic field.

In contrast, neutrons that are created near the midplane via (p, n) reactions are typically stopped only if they traverse $\sim$50 g cm^{-2} of the target rocks. The magnetic field exerts no confining influence on them, so neutrons will escape (and decay) in the vertical direction if the disk contains a local surface density significantly less than 50 g cm^{-2}. With $F = 0.01$, $X_r = 4 \times 10^{-3}$, $\Delta t \sim 10$ yr, $R_x \sim 1 \times 10^{12}$ cm, and $\Delta R \sim 0.25 R_x$, we estimate that the average surface density of rocks in the reconnection ring, $F X_r \dot{M}_D \Delta t/2\pi R_x \Delta R$, is, at best, $\sim$1 g cm^{-2}, even if $\dot{M}_D$ has the relatively large value $\sim 2 \times 10^{-6}\, M_\odot$ yr^{-1} that applies to embedded protostars. Thus, even during the main epoch of CAI formation (see Shu et al. 1996, 1997), secondary neutrons have only about one chance in 50 of being captured before they escape from the layer of rock within which they are generated. This relatively small capture probability justifies in a first treatment our neglect of the transformations induced by secondary neutrons compared to those induced by primary cosmic-ray ions. (See, however, § 6 for a discussion of a different case, in which the underlying target is truly thick to both ions and neutrons.)

4. PRODUCTION OF ^{41}Ca, ^{53}Mn, ^{138}La, AND ^{50}V BY PROTON AND α REACTIONS

We begin by adopting $q = 0.7$ and $p = 3.5$ for impulsive flares triggered by magnetic reconnection in the reconnection ring. Figure 12 of Ramaty et al. (1996) gives the energy-dependent cross sections for making ^{26}Al, ^{41}Ca, and ^{53}Mn from likely reactions involving protons and α-particles. In Figure 3 we show similar cross sections computed by statistical (Hauser-Feshbach) model codes for the production of some other nuclides of interest. The calculations were done with one of two programs, ALICE (Blann 1966) or PACE (Gavron 1980). Experimental data measured for neighboring nuclei guided our choices for the input parameters of the model computations. A comparison of the statistical codes with experimental data for known systems (see, e.g., Schopper 1991) in the mass range $A = 24$–65 shows good agreement (better than a factor of 2) for strong reaction channels with peak $\sigma > 100$ mbarn. Based on these comparisons, we chose PACE for reactions involving lighter nuclei (e.g., ^{24}Mg or ^{40}Ca) and ALICE for heavier nuclei (e.g., ^{48}Ti or ^{138}Ba). For weaker channels, deviations

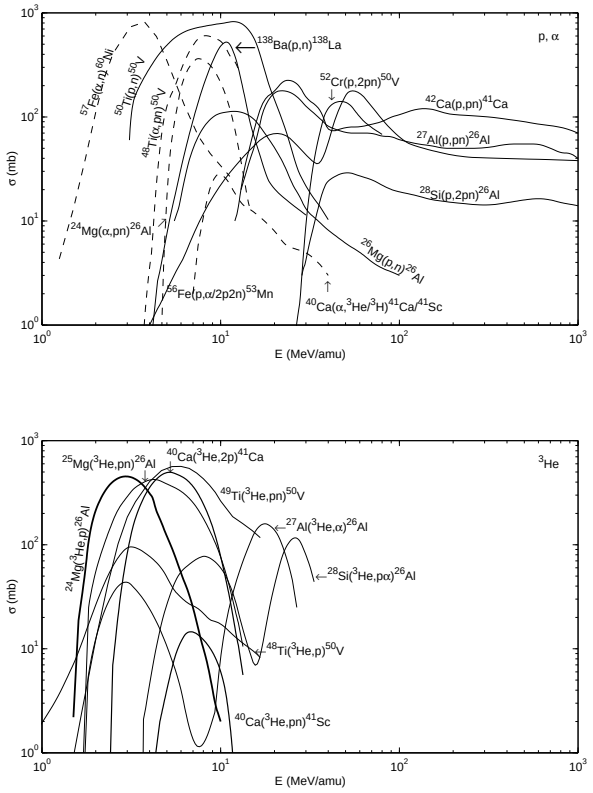

FIG. 3.—Adopted cross sections for the reactions considered in this paper. The upper panel gives proton cross sections (*solid lines*) and α reactions (*dashed lines*). The lower panel gives cross sections for ^{3}He reactions, with heavier lines denoting the pathways for producing ^{26}Al and ^{41}Ca discussed at length in the text.

of up to an order of magnitude have been observed, particularly at energies well below the peak. The situation is sometimes confused by the experimental data, themselves differing by factors up to 3 (especially at low energies), measured by different groups. Within such uncertainties, the corresponding values for $\mathscr{B}(p = 3.5)$ are listed in the third column of Table 2.

Since argon and potassium are volatile in the precursor rocks found in the reconnection ring, the most important channels for producing ^{41}Ca are ^{42}Ca(p, pn)^{41}Ca ($\mathscr{B} = 1.2$) and ^{40}Ca(α, ^{3}He)^{41}Ca or ^{40}Ca(α, ^{3}H)^{41}Sc, which electron-captures to ^{41}Ca ($\mathscr{B} = 0.17$ for both reactions). The first target ^{42}Ca has an abundance ratio $x_T^r/x_S^r = 6.7 \times 10^{-3}$ relative to the dominant calcium isotope ^{40}Ca (Anders & Ebihara 1982), while the projectile in the second and third reactions corresponds to $(A/Z^2)_{CR} = 1$ and $y_{CR} = 0.1$ if α-particles have the same ratio to protons as cosmic helium does to hydrogen. If we sum the three contributions, equation (20) yields $^{41}\mathrm{Ca}/^{40}\mathrm{Ca} = 1.1 \times 10^{-4}\epsilon_{10}$, which agrees with the value inferred for $^{41}\mathrm{Ca}/^{40}\mathrm{Ca}$ in Efremovka CAIs listed in Table 1 (Srinivasan et al. 1994) if $\epsilon_{10} = 1.4 \times 10^{-4}$. (The more general requirement is $\epsilon_{10}/F = 1.4 \times 10^{-2}$.) This requirement for ϵ_{10} as a time average for impulsive flares is quite compatible with equation (7).

The large iron-to-manganese ratio in CAI and chondrule precursors makes ^{56}Fe the primary target for the spallation production of ^{53}Mn. Experiments for proton-induced spallation reactions on ^{56}Fe at effective energies between 100 and 580 MeV (Lau, Mewalt, & Stone 1985) give ^{53}Fe yields (which become ^{53}Mn by electron capture on a timescale of

TABLE 2

$\mathscr{A}$ AND $\mathscr{B}$

Reaction	$\mathscr{A}(p = 2.7)$	$\mathscr{B}(p = 3.5)$
^{26}Mg(p, n)^{26}Al	1.2	1.0
^{27}Al(p, pn)^{26}Al	3.2	0.92
^{28}Si(p, $2pn$)^{26}Al	0.63	0.10
^{24}Mg(α, pn)^{26}Al	2.0	2.5
^{28}Si(α, αpn)^{26}Al	1.1	0.41
^{42}Ca(p, pn)^{41}Ca	4.6	1.2
^{40}Ca(α, ^{3}He)^{41}Ca	0.20	0.17
^{40}Ca(α, ^{3}H)^{41}Sc	0.20	0.17
^{50}Ti(p, n)^{50}V.....	11.	13.
^{51}V(p, $2n$)^{50}V	3.2	1.5
^{52}Cr(p, $2pn$)^{50}V	0.94	0.26
^{48}Ti(α, pn)^{50}V	4.0	4.8
^{56}Fe(p, $p3n$)^{53}Fe	0.18	0.024
^{56}Fe(p, $2p2n/\alpha$)^{53}Mn.....	2.8	0.82
^{53}Cr(p, n)^{53}Mn	11.	11.
^{57}Fe(α, n)^{60}Ni	5.1	12.
^{138}Ba(p, n)^{138}La	2.6	2.5
^{24}Mg(^{3}He, p)^{26}Al	3.6	9.5
^{25}Mg(^{3}He, pn)^{26}Al.....	4.4	8.8
^{27}Al(^{3}He, α)^{26}Al	1.2	1.3
^{28}Si(^{3}He, $p\alpha$)^{26}Al.....	1.1	0.96
^{40}Ca(^{3}He, $2p$)^{41}Ca	4.0	6.8
^{48}Ti(^{3}He, p)^{50}V	0.94	2.0
^{49}Ti(^{3}He, pn)^{50}V	6.4	10.
^{50}Ti(^{3}He, $p2n$)^{50}V.....	4.9	4.1

∼2 yr) that are smaller by a factor ∼4 than those adopted by Ramaty et al. (1996). The more important channels to ^{53}Mn production from ^{56}Fe are the direct routes, ^{56}Fe(p, α)^{53}Mn and ^{56}Fe(p, $2p2n$)^{53}Mn, for which we use the experimental cross sections measured by Gensho et al. (1979; see also Fig. 3). Manganese and iron are similar in volatility; therefore we adopt cosmic abundances for the preirradiation $^{56}\mathrm{Fe}/^{55}\mathrm{Mn} = 87$ (Anders & Ebihara 1982). With $\mathscr{B} = 0.024$ for the first reaction and $\mathscr{B} = 0.82$ for the sum of the second two reactions, the total contribution to ^{53}Mn production from proton-induced reactions on ^{56}Fe gives an expected $^{53}\mathrm{Mn}/^{55}\mathrm{Mn} = 0.20\epsilon_{10}$. This is compatible with the corresponding entry in Table 1 (Birck & Allégre 1985) if ϵ_{10} for reaction-inducing impulsive flares has the value 1.4×10^{-4} that we inferred from the production of ^{41}Ca.

Partial support for the choice $\epsilon_{10} = 1.4 \times 10^{-4}$ in impulsive flares comes from the search for ^{138}La excess in meteorites. This long-lived isotope (mean life $> 10^{12}$ yr) cannot be made inside stars by thermal proton capture or by neutron capture in either the *r*- or *s*-processes (see Fig. 1 in Shen, Lee, & Chang 1994). A fragile nucleus with odd numbers of neutrons and protons, it will typically be destroyed by photodissociation before much of it can be created by energetic photon processes such as ^{139}La(γ, n)^{138}La. Whole rock samples of the Murchison and Allende carbonaceous chondrites show tantalizing, marginally significant, excesses of 0.12% for $^{138}\mathrm{La}/^{139}\mathrm{La}$ (Shen et al. 1994). In contrast, with a 2 σ detection limit of 0.08%, Shen et al. found no excess $^{138}\mathrm{La}/^{139}\mathrm{La}$ in whole rock samples of ordinary chondrites compared to the terrestrial standard.

A viable mechanism for generating ^{138}La is by the cosmic-ray reaction ^{138}Ba(p, n)^{138}La. Figure 3 gives our estimate of the cross section for this reaction, which corresponds to a value of $\mathscr{B} = 2.5$. With $^{138}\mathrm{Ba}/^{139}\mathrm{La} = 7.0$ (Anders & Ebihara 1982), $(A/Z^2)_{CR} = 1 = y_{CR}$, and $\epsilon_{10} = 1.4 \times 10^{-4}$, equation (20) predicts $^{138}\mathrm{La}^*/^{139}\mathrm{La} = 6.6 \times 10^{-6}$. This represents a ^{138}La excess that is 0.74% of the canonical ratio, $^{138}\mathrm{La}/^{139}\mathrm{La} = 9 \times 10^{-4}$ (Anders &

Ebihara 1982). We may compare this value with direct measurements of the ^{138}La excess in CAIs by Shen, Ho, & Lee (1998), who were motivated to make these measurements by our calculation. Four out of six CAIs they analyzed show ^{138}La excesses between 0.26% and 0.61%, clearly resolvable from their terrestrial standard since their 2 σ detection limit is 0.16%. These values are consistent with our prediction if the proton irradiation of CAIs is somewhat variable, with some CAIs receiving less than full dosages. Unfortunately, examination of the CAIs with low ^{138}La*/^{139}La for their ^{26}Mg*/^{27}Al content by G. R. Huss & G. J. Wasserburg (1998, private communication), again carried out at our request, shows the normal inference, ^{26}Al/^{27}Al $= 5 \times 10^{-5}$. Thus, either the irradiation genesis of ^{26}Al is somewhat decoupled from that of ^{138}La (see below), or natural variations of the ^{138}La/^{139}La ratio because of inhomogeneous stellar nucleosynthesis have masked any protosolar cosmic-ray production.

To obtain a different test, we calculate the production yield by cosmic-ray bombardment of a similar odd-odd nucleus, ^{50}V. From the perspective of reasonable cross sections and relative abundances (see Fig. 3), the most favorable proton or α reactions are ^{48}Ti(^{4}He, pn)^{50}V ($\mathscr{B} = 4.8$), ^{50}Ti(p, n)^{50}V ($\mathscr{B} = 13$), ^{51}V(p, $2n$)^{50}V ($\mathscr{B} = 1.5$), and ^{52}Cr(p, $2pn$)^{50}V ($\mathscr{B} = 0.26$). With ^{48}Ti/^{51}V $= 6.0$, ^{50}Ti/^{51}V $= 0.43$, ^{52}Cr/^{51}V $= 38$ (Anders & Ebihara 1982), and $\epsilon_{10} = 1.4 \times 10^{-4}$, equation (20) then predicts a synthesis ratio of ^{50}V*/^{51}V $= 7.5 \times 10^{-6}$ in fully irradiated CAIs. This represents an excess of 0.30% compared to the normal ^{50}V/^{51}V $= 2.5 \times 10^{-3}$ (Anders & Ebihara 1982). Detection of such an excess is within the capabilities of current experimental technique.

The story for chondrules may be different. During the embedded stage, most protochondrules that continue to drift by plasma drag fully into the reconnection ring or farther will evaporate upon launch by an encroaching x-wind, adding their calcium-aluminum–rich phases to the formation of CAIs (Shu et al. 1996). Lower values than those cited above (but still nonzero) for ^{41}Ca/^{40}Ca, ^{53}Mn/^{55}Mn, ^{138}La*/^{139}La, and ^{50}V*/^{51}V should hold in chondrules that survive heating in the x-wind after partial irradiation in the transition zone between the x-region and the reconnection ring.

5. PRODUCTION OF ^{26}Al, ^{41}Ca, AND ^{50}V BY ^{3}He REACTIONS

The dominant reactions for making ^{26}Al by proton and α bombardment of refractory rocks in impulsive flares are ^{27}Al(p, pn)^{26}Al ($\mathscr{B} = 0.92$), ^{26}Mg(p, n)^{26}Al ($\mathscr{B} = 1.0$), ^{24}Mg(α, pn)^{26}Al ($\mathscr{B} = 2.5$ and $y_{CR} = 0.1$), ^{28}Si(p, $2pn$)^{26}Al ($\mathscr{B} = 0.10$), and ^{28}Si(α, αpn)^{26}Al ($\mathscr{B} = 0.41$). With ^{27}Al/^{27}Al $= 1$, ^{26}Mg/^{27}Al $= 1.4$, ^{24}Mg/^{27}Al $= 10$, and ^{28}Si/^{27}Al $= 11$ (Anders & Ebihara 1982), equation (20) yields the sum of the five contributions to ^{26}Al/^{27}Al as $1.7 \times 10^{-2} \epsilon_{10}$. If $\epsilon_{10} = 1.4 \times 10^{-4}$ in impulsive flares, the result is 20 times lower than the value inferred for CAIs (see Table 1).

This result is insensitive to the assumed cosmic-ray energy spectrum. We have carried out the same computations assuming that gradual flares with $p = 2.7$ are the dominant mechanism of proton and α acceleration in the reconnection ring. The corresponding values for $\mathscr{A}(p = 2.7) = \mathscr{B}(p = 2.7)$ are listed in the second column of Table 2. For proton and α irradiation by gradual flares, we compute ^{41}Ca/^{40}Ca $= 1.5 \times 10^{-8}$, ^{53}Mn/^{55}Mn $= 5.4 \times 10^{-5}$, and ^{138}La*/^{139}La $= 5.2 \times 10^{-6}$ if $\epsilon_{10} = 1.1 \times 10^{-4}$ for such gradual flares. This is again consistent with the measured values, but the same choice for ϵ_{10} produces a ratio ^{26}Al/^{27}Al by proton and α reactions that is 16 times lower than the canonical meteoritic value. Clearly, ^{26}Al cannot be made mostly by proton and α bombardment of neighboring nuclides in the periodic table if ^{41}Ca, ^{53}Mn, and ^{138}La are also made by such bombardment (see also Goswami, Marhas, & Sahijpal 1996).

In impulsive flares, ^{3}He is preferentially accelerated to MeV energies, probably by resonant particle-wave interactions in magnetic reconnection events because ^{3}He^{++} is the only ionic species whose gyrofrequency lies between those of ^{1}H$^+$ and ^{4}He^{++} (Fisk 1978; Temerin & Roth 1992). Above $\sim$1 MeV nucleon^{-1}, the abundance of ^{3}He can exceed that of α-particles (0.1 relative to protons), sometimes by a factor of as much as 10 (see Fig. 8 of Reames et al. 1997); i.e., for nucleosynthetic purposes, ^{3}He ions can be as numerous as protons. The reaction ^{24}Mg(^{3}He, p)^{26}Al is especially interesting because it is exothermic (by 5.9 MeV) and therefore lacks a threshold. The very large numbers of low-energy cosmic-ray ^{3}He nuclei in impulsive flares can then help make ^{26}Al as long as this advantage is not offset by the increasing scattering and ionization losses in the rock and by the increasing importance of Coulomb barriers at small energies.

We have performed Hauser-Feshbach calculations for the reaction cross section of ^{24}Mg(^{3}He, p)^{26}Al, as well as the additional contributors: ^{28}Si(^{3}He, αp)^{26}Al, ^{25}Mg(^{3}He, pn)^{26}Al, and ^{27}Al(^{3}He, α)^{26}Al. The results are shown in Figure 3. Our theoretical estimate for ^{24}Mg(^{3}He, p)^{26}Al is in good agreement with a scaling of the experimental cross section measured at moderate energies for the closely analogous reaction ^{26}Mg(^{3}He, p)^{28}Al (see Frantsvog et al. 1982, especially their Fig. 1). For solar impulsive flares, the ^{3}He spectrum can be reasonably approximated as a power law, $y_{CR}\, dN_p/dE \propto E^{-3.5}$ for $E \geq 1$ MeV amu^{-1}, but the spectra in different flares do show variation, as well as generally having some curvature, being shallower ($p < 3.5$) at lower energies and steeper ($p > 3.5$) at higher energies (see Fig. 9 of Reames et al. 1997). With p taken to be 3.5 for $E \geq 1$ MeV amu^{-1}, equation (21) now yields $\mathscr{B} = 9.5$, 0.96, 8.8, and 1.3 for ^{24}Mg(^{3}He, p)^{26}Al, ^{28}Si(^{3}He, αp)^{26}Al, ^{25}Mg(^{3}He, pn)^{26}Al, and ^{27}Al(^{3}He, α)^{26}Al, respectively. With ^{24}Mg/^{27}Al $= 10$, ^{28}Si/^{27}Al $= 11$, ^{25}Mg/^{27}Al $= 1.3$, and $(A/Z^2)_{CR} = \frac{3}{4}$, equation (20) gives ^{26}Al/^{27}Al $= 0.26 \epsilon_{10}\, y_{CR}$. We can therefore reproduce the value listed in Table 1 if $\epsilon_{10}\, y_{CR} = 1.9 \times 10^{-4}$ in protostellar impulsive flares, which yields a required ratio of ^{3}He to protons, $y_{CR} = 1.4$, if ϵ_{10} for impulsive flares in the reconnection ring equals the value 1.4×10^{-4} needed to make meteoritic levels of ^{41}Ca, ^{53}Mn, and ^{138}La. This value for y_{CR} is formally a little large, but it is not yet troublesome given the uncertainties in the theoretical cross sections and in the exact shape of the ^{3}He cosmic-ray spectrum. For example, the same ratios of ^{26}Al/^{27}Al (by ^{3}He reactions) relative to those of ^{41}Ca/^{40}Ca, ^{53}Mn/^{55}Mn, and ^{138}La*/^{139}La (by proton and α reactions) can be achieved with $y_{CR} = 0.47$, if the energy spectrum for protosolar impulsive flares is somewhat steeper than for modern flares: $p = 4.0$ instead of 3.5.

With $p = 3.5$ and $\epsilon_{10}\, y_{CR} = 1.9 \times 10^{-4}$, we estimate that ^{3}He reactions in impulsive flares do not compete with proton and α reactions in impulsive flares for producing ^{53}Mn and ^{138}La. The situation is different for ^{50}V and

^{41}Ca. The most important ^{3}He reactions for producing ^{50}V are ^{48}Ti(^{3}He, p)^{50}V ($\mathscr{B} = 2.0$ for $p = 3.5$), ^{49}Ti(^{3}He, pn)^{50}V ($\mathscr{B} = 10$), and ^{50}Ti(^{3}He, $p2n$)^{50}V ($\mathscr{B} = 4.1$). With ^{48}Ti/^{51}V = 6.0, ^{49}Ti/^{51}V = 0.44, ^{50}Ti/^{51}V = 0.43, $A/Z^2 = 3/4$, and $\epsilon_{10}\, y_{CR} = 1.9 \times 10^{-4}$, equation (20) yields the ^{3}He contribution to the production of excess ^{50}V as ^{50}V*/^{51}V $= 7.4 \times 10^{-6}$, which is 0.30% of the normal ratio of ^{50}V/^{51}V, comparable to the proton and α contribution that we computed earlier.

Consider now the case of ^{41}Ca. The most important reactions involve transfers: ^{40}Ca(^{3}He, $2p$)^{41}Ca, ^{40}Ca(^{3}He, ^{2}H)^{41}Sc, and ^{40}Ca(^{3}He, np)^{41}Sc, with ^{41}Sc electron-capturing to ^{41}Ca. The first reaction is slightly exothermic (by 0.64 MeV), whereas the second and third reactions are endothermic (by 4.4 and 6.6 MeV, respectively). Thus, we anticipate the second and third reactions to contribute negligibly compared to the first. This suspicion is confirmed by our Hauser-Feshbach calculations for these reactions, summarized in Figure 3. For ^{40}Ca(^{3}He, $2p$)^{41}Ca, we get $\mathscr{B} = 6.8$. If $\epsilon_{10}\, y_{CR} = 1.9 \times 10^{-4}$, equation (20) implies ^{41}Ca/^{40}Ca $= 2.6 \times 10^{-6}$. The predicted ratio for ^{41}Ca/^{40}Ca is 2 orders of magnitude larger than shown in Table 1. How can we reconcile this discrepancy?

Shu et al. (1997) proposed a possible solution if proto-CAIs have "thick mantles of less refractory rock surrounding more refractory cores. Then, ^{3}He nuclei of a few MeV per nucleon are stopped in an outer rock layer of thickness ~ 60 μm after they have had a chance to interact with the target atom's ^{24}Mg for producing ^{26}Al, but before they have penetrated the core to interact with the target atom's ^{40}Ca for producing ^{41}Ca. Upon launch in the x-wind, the ^{26}Al atoms will diffuse to the calcium-aluminum–rich core, whereas most of the magnesium-rich mantle evaporates away, leaving the thin rims found on normal CAIs." Protons and α-particles with energies in the tens of MeV amu^{-1} needed to initiate the reactions discussed in § 4 for producing ^{41}Ca and ^{53}Mn would still make it into the core of the CAI, but ^{138}La* and ^{50}V* yields by the lower energy reactions involving protons, α-particles, or ^{3}He particles would be reduced from the values calculated in this paper. Unfortunately, the heating of CAIs to temperatures near 1800 K upon their launch in the x-wind would probably erase spatial gradients as a useful diagnostic of this shielding effect.

A more conventional solution appeals to reequilibration after the decay of the parent radionuclide, as in the usual explanation for the lack of ^{26}Mg*/^{27}Al in some normal CAIs (see the second peak near 0 in Fig. 1). Extensive invasion of alkali-rich material through thermal diffusion or transport by flowing water did take place in some Allende CAIs after their initial resolidification at high temperatures when they were naturally deficient in alkali metals (Grossman 1980). Srinivasan et al. (1994) cite an undisturbed magnesium system in the two Efermovska CAIs they measured as supporting evidence for an undisturbed value of the ^{41}Ca/^{40}Ca ratio listed in Table 1. However, potassium is much more mobile in rock than is magnesium, and it may be possible to reequilibrate the decay product of ^{41}Ca without altering that of ^{26}Al. The potassium depletion required to see ^{41}Ca decay is so extreme that even a minute amount of mixing may be enough to mask the true excess of ^{41}K from ^{41}Ca decay.

As a final alternative, if gradual flares rather than impulsive flares provide the dominant irradiation mechanism, ^{3}He reactions may not contribute to the production of radionuclides. Then ^{41}Ca, ^{53}Mn, and ^{138}La can be made at their inferred CAI levels by proton and α irradiation within the solar system, but ^{26}Al would need to come from a Galactic source.

6. THE DIFFICULT CASE OF ^{60}Fe

The radionuclide ^{60}Fe presents another difficulty. It is highly neutron rich ($\Delta N = 8$), which makes it almost impossible to synthesize by cosmic-ray reactions. On the one hand, reactions that have reasonably large cross sections involve targets or projectiles that are themselves neutron rich, which implies that they have relatively small cosmic abundances (because their production requires special nucleosynthetic sites inside stars). On the other hand, targets or projectiles that are relatively abundant (and therefore not especially neutron rich) have very small cross sections for making ^{60}Fe. A detailed examination in Appendix B of many charged-particle reactions leads to the conclusion that the reconnection-ring mechanism falls short of making the required ^{60}Fe by 2 or more orders of magnitude. If ^{60}Fe was indeed live in the early solar system at the level indicated in Table 1, then this radionuclide presents almost incontrovertible evidence for external injection by a neutron-rich stellar source. [The multistep neutron-capture process, (p, n) reactions plus ^{58}Fe(n, γ)^{59}Fe(n, γ)^{60}Fe, is completely negligible in the context of the reconnection-ring model.]

However, the inference for live ^{60}Fe in the early solar system arises from trace amounts of excess ^{60}Ni that correlate imperfectly with ^{56}Fe in stony meteorites called eucrites (see the reference in Table 1). The parent body of eucrites is thought to be Vesta, where the nickel in the surface rocks (destined to become the meteorites in some asteroidal collision process) has been separated from the iron during the core formation of this differentiated asteroid. Irradiation of the resulting basaltic rocks on the surface of Vesta by SEPs will lead to a ^{60}Ni excess that correlates with ^{56}Fe if the target is any of the stable isotopes of iron. The correlation will be imperfect, however, because of different levels of shielding by the overlying rock. In any case, small excesses are possible to measure in minerals that have very depleted ratios of Ni/Fe.

The surface rocks would be repeatedly tilled by sporadic impacts, so the effective irradiation depth may reach much deeper than the formal penetration depth of protons with energies ~ 10 MeV. Eucrites exhibit widespread evidence of brecciation, which supports the notion of gardening by meteoroid impacts. Later burial of the irradiated surface rocks may anneal the accompanying ionization tracks. Warren (1991) has studied the temperature history of differentiated asteroids. By extensive modeling of the heat released by the interior of planetesimals that melt and differentiate into metallic cores and silicate mantles, he shows that the crusts will remain at temperatures in excess of 1000 K for 10–200 Myr for a wide range of assumed parameters. Since eucrites probably come from the lower portion (cumulates and gabbros) of the crust of Vesta, the annealing of cosmic-ray tracks presents no difficulty. The same heating could outgas the rare isotopes of noble gases, such as ^{21}Ne; thus, cosmic-ray exposures estimated on the basis of these diagnostics for eucrites may not give a true picture of the first 100 Myr history of Vesta, when it suffered heavy bombardment by meteoroids and SEPs. This claim is

consistent with the results of Wooden et al. (1979), who find an age of considerably less than 4.56 Gyr for Chervony Kut based on Ar-Ar dating.

We have examined this problem and conclude that the most favorable reaction is ^{57}Fe(α, n)^{60}Ni (see Fig. 3). An approximate estimate for the production ratio of radionuclide R to stable isotope S can be obtained by dividing equation (18) by the number per unit area, $x_S^r \Sigma_p^r(E_{10})/m_r$, of S atoms within a rock stopping column for protons of energy $E_{10} = 10$ MeV, after we replace $\dot{N}_p \Delta t$ by the fluence (time integrated number flux) $\mathscr{F}_p(E_{10})$ of protons with energy $\geq E_{10}$:

$$\frac{N_R}{N_S} = (q+1)\mathscr{A} y_{\rm CR} \frac{x_T^r}{x_S^r} \left(\frac{A}{Z^2}\right)_{\rm CR} \sigma_0 \mathscr{F}_p(E_{10}) . \qquad (22)$$

Gradual flares associated with CMEs on open field lines generate most of the protons and α-particles that escape to interplanetary space. With $p = 2.7$ and $q = 0.7$, equation (17) yields $\mathscr{A} = 5.1$ for the reaction ^{57}Fe(α, n)^{60}Ni. With $x_T^r/x_S^r = {}^{57}\text{Fe}/{}^{56}\text{Fe} = 0.023$, $y_{\rm CR} = 0.1$, equation (22) now gives ^{60}Ni*/^{56}Fe $= 2.0 \times 10^{-27} \mathscr{F}_p(E_{10})$. This formula agrees with Chervony Kut if $\mathscr{F}_p(E_{10}) = 2.0 \times 10^{18}$ cm^{-2} (Shukolyukov & Lugmair 1993a), whereas it agrees with Juvinas if $\mathscr{F}_p(E_{10})$ is 10 times lower (Shukolyukov & Lugmair 1993b). Such fluence levels are compatible with estimates of the minimum value of $\mathscr{F}_p(E_{10}) = 4 \times 10^{17}$ cm^{-2} needed to explain the ^{21}Ne measured in "gas-rich" meteorites (Caffee et al. 1987, 1991). The differences between Chervony Kut and Juvinas may be attributable to the depth at which their parent material was buried beneath the surface at the time that the primary irradiation took place.

The thermal-neutron–capture cross section associated with ^{149}Sm(n, γ)^{150}Sm is about 40,000 barn. But Shukolyukov & Lugmair (1993a, p. 1139) point out that the ratio ^{150}Sm/^{149}Sm in Chervony Kut is normal, which places an upper limit on the neutron fluence of 1×10^{15} cm^{-2}. Do the neutrons released by our scheme (fast initially, but eventually slowed down by the interior rock of Vesta), ^{57}Fe(α, n)^{60}Ni, violate this upper limit?

Of the α fluence, $y_{\rm CR} \mathscr{F}_p(E_{10}) = 2.0 \times 10^{17}$ cm^{-2}, required to generate the measured ^{60}Ni*/^{56}Fe level in Chervony Kut, a fraction $\eta_{\rm TR}^r$ given by equation (15) produces neutrons via ^{57}Fe(α, n)^{60}Ni. With the data presented earlier, we easily compute $\eta_{\rm TR}^r = 9.6 \times 10^{-5} x_S^r$, where x_S^r is the number fraction of ^{56}Fe in the basaltic rock of Chervony Kut. The sample with highest significance (bulk 3) has $x_S^r = 0.15$, in which case the associated neutron fluence is 2.9×10^{12} cm^{-2}, well below the upper limit set by ^{150}Sm/^{149}Sm.

The most important source of free neutrons of the reactions considered in this paper is from ^{56}Fe(p, $2p2n$)^{53}Mn, for which we estimate $\eta_{\rm TR}^r = 1.8 \times 10^{-3} x_S^r$, where x_S^r is again the ^{56}Fe number fraction 0.15 in bulk 3. With a proton fluence $\mathscr{F}_p(E_{10}) = 2.0 \times 10^{18}$ cm^{-2}, the associated neutron fluence $2\eta_{\rm TR}^r \mathscr{F}_p(E_{10})$ is 1.1×10^{15} cm^{-2}, equal to the upper limit set by ^{150}Sm/^{149}Sm.

The complete problem is considerably more complicated and might be interesting to pursue in the future both experimentally and theoretically. There are probably many (p, n) reactions for releasing free neutrons that are competitive with or even somewhat more important than those considered above. The neutrons produced, however, will initially be more energetic than those that give the peak (resonant-capture) cross section for ^{149}Sm. How these neutrons are absorbed and scattered by nuclei much more abundant than ^{149}Sm before they acquire suitable energies for preferential capture by ^{149}Sm requires a complex calculation in neutron transport theory. The main point we wish to make here is merely that the total production yield of secondary neutrons probably does not give any immediate contradictions with the available data.

Are proton fluences of the magnitude $\mathscr{F}_p(E_{10}) = 2.0 \times 10^{18}$ cm^{-2} reasonable from other astrophysical points of view? Weak-lined T Tauri stars (WTTSs) and post–T Tauri stars (PTTSs) are believed to be pre–main-sequence stars of sunlike masses that have largely dispersed their nebular disks (Bertout 1989; Martin 1997). They have typical X-ray luminosities of 3×10^{29} ergs s^{-1} (Feigelson et al. 1987; Neuhäuser 1997). If we assume the same scaling for fast protons as adopted elsewhere in this paper, we estimate that WTTSs and PTTSs emit $\sim 7 \times 10^{32}$ protons second^{-1} with energy above 10 MeV nucleon^{-1}. Spread out over a sphere of radius 2.5 AU, this amounts to a number flux of $\sim 4 \times 10^4$ cm^{-2} s^{-1}.[2] Such a number flux accumulates to a fluence $\mathscr{F}_p(E_{10}) = 2.0 \times 10^{18}$ cm^{-2} in 1.6 Myr. The WTTS plus PTTS stages of pre–main-sequence evolution may last 30 Myr, and young sunlike stars may remain reasonably X-ray active to ages of ~ 500 Myr (Magazzu et al. 1997; Martin 1998; Randich 1998). The irradiation of meteoritic parent bodies whose surfaces are continually tilled over such periods of time may therefore extend effectively to almost a meter in depth.

Gradual-flare bombardment of surface rocks on asteroids contributes negligible production of ^{26}Al (which requires irradiation by ^{3}He) but formally nonnegligible amounts of ^{41}Ca, ^{53}Mn, and ^{138}La in an exposed CAI. For the same set of reactions as considered in § 4, equation (22) yields ^{41}Ca/^{40}Ca $= 2.4 \times 10^{-8}$, ^{53}Mn/^{55}Mn $= 8.9 \times 10^{-5}$, and ^{138}La*/^{139}La $= 6.2 \times 10^{-6}$ for a proton fluence $\mathscr{F}_p(E_{10}) = 2.0 \times 10^{18}$ cm^{-2}. Thus, if CAIs experienced a proton and α dosage comparable to that needed to explain the ^{60}Ni anomaly in Chervony Kut, irradiation of a surface layer of rocks on the appropriate meteoritic parent bodies could explain, in principle, the complete list of extinct radionuclides more short-lived than ^{107}Pd in Table 1, except for ^{26}Al.

The actual situation is again more complex. The concentrations of live ^{41}Ca and ^{53}Mn will reach equilibrium between production and decay if the irradiation occurs over many Myr, and the decay products ^{41}K and ^{53}Cr may migrate to other sites if the underlying rock gets hot enough to anneal cosmic-ray tracks. The resulting values of ^{41}K*/^{40}Ca and ^{53}Cr*/^{55}Mn will then be lower than indicated by equation (22). The same argument does not apply to metastable and highly refractory ^{138}La. Thus, the documented case of ^{21}Ne production by solar-system irradiation of the parent bodies of gas-rich meteorites (usually carbonaceous chondrites) implies that the same process may introduce fairly large fluctuations on top of the ratio ^{138}La*/^{139}La

[2] The assumption of free propagation through space is naive, since cosmic-ray ions interact with the time-varying magnetic field of the solar wind. Mechanisms exist (adiabatic decompression, collisionless shock waves, etc.) that can either decrease or increase the original energies of the particles. It is beyond the scope of the present paper to attempt any estimates for the net effect of such processes.

established in CAIs by any prior mechanism (external stellar seeding, reconnection-ring irradiation, etc.). To be sure, this explanation seems to imply that the rocks of ordinary chondrites exposed to such irradiation ought also to have shown ^{138}La excesses compared to the terrestrial standard, whereas Shen et al. (1994) found none. The difficulty may not be acute, since the measurements were made on bulk samples, which would tend to dilute any real effects.

Except for ^{60}Fe (and some fluctuations in ^{138}La*), we prefer the explanation offered by the reconnection-ring mechanism because of its much greater efficiency for producing short-lived radionuclides. The reconnection-ring mechanism allows the irradiation of almost all the rocks known to be present in the solar system, whereas the irradiation of the asteroids after the solar nebula has cleared allows the ratios in Table 1 for ^{41}Ca/^{40}Ca and ^{53}Mn/^{55}Mn to be established, at best, only for a surface layer of exposed rocks. Most importantly, assuming that chondrules are partially irradiated in the reconnection ring to a typical level ^{26}Al/^{27}Al $= 9 \times 10^{-6}$ by ^{3}He impulsive flares, ^{26}Al would exist in sufficient quantities to act as the ubiquitous heat source that melted many asteroids within a few million years of their assemblage (Shukolyukov & Lugmair 1993a, 1993b; LaTourette & Wasserburg 1998).

7. DISCUSSION

To close the arguments of this paper, we point to the following astrophysical arguments for synthesizing ^{26}Al internally to the solar system.

1. In external seeding scenarios, peculiar abundances of stable nuclides should have been imported along with the extra ^{26}Al. Thus, one might have expected samples rich in ^{26}Al to show large anomalies in stable isotopes as well. The most extreme stable anomalies actually occur in the FUN inclusions, which however exhibit only low ^{26}Al/^{27}Al ratios (Clayton, Hinton, & Davis 1988). The anticorrelation is explained in the fluctuating x-wind model by FUN inclusions belonging to the group of unirradiated CAIs that never entered the reconnection ring from the x-region. They experienced only brief heating to $\sim$1800 K for tens of hours when lifted by the x-wind (Shu et al. 1996). These FUN inclusions would then have a chance of retaining presolar anomalies that would be wiped out in normal CAIs by their extended heat treatment and plasma-solid exchange in the reconnection ring, lasting for decades.

2. Launch in the x-wind without experiencing irradiation in the reconnection ring may also account for the population of CAIs and chondrules with no detectable ^{26}Mg* (MacPherson et al. 1995; Russell et al. 1996; Lee et al. 1977; Hutcheon, Huss, & Wasserburg 1994; Hutcheon & Jones 1995).[3] This picture would provide an alternative explanation to equilibration between Mg-rich and Mg-poor phases for the bimodal distributions seen in Figure 1. To make the ^{26}Mg atoms sufficiently mobile in the equilibration model, CAIs need to be heated to $\geq$1000 K several million years after CAIs trapped the original ^{26}Al. This heating probably occurred on parent bodies large enough ($\gtrsim$15 km) to contain the energy released by the radioactive decay of ^{26}Al itself (LaTourette & Wasserburg 1998). In order for the surrounding matrix material not to be affected, nebular dust would need to be swept into the body's regolith after the surface of the parent body has cooled to below a few hundred K. In such a scenario, it is much easier to reset the ^{41}Ca clock than it is to reset the ^{26}Al clock.

3. If all solar system material were initially seeded at a level ^{26}Al/^{27}Al $= 5 \times 10^{-5}$, CAIs must be made $\sim$5 Myr before ^{26}Al-free chondrules (Russell et al. 1996). Because of gas drag, centimeter-sized CAIs drift inward from the asteroid belt on timescales of only $\sim 10^4$ yr (Cameron 1995; Whipple 1972; Weidenschilling 1977; Cuzzi, Dubrovolskis, & Champney 1993; Wood 1996). To prevent their falling into the sun for $\sim$5 Myr, they need to accrete onto planetesimals of size 10^4 cm or larger. To reset the clock in CAIs for which no ^{26}Al is inferred, a comparable duration of time has to pass before the asteroid cooled to below 1000 K, and matrix material must be added after the surface has cooled to below a few hundred K. However, the best astronomical evidence suggests that dusty nebular disks survive around young sunlike stars for only 1–3 Myr (Hartmann et al. 1997; Martin 1998). Production of different levels of ^{26}Al/^{27}Al in CAIs and chondrules by cosmic-ray bombardment in the early solar system relaxes the time required to pass to $\gtrsim$0.7 Myr before the ^{41}Ca clock in CAIs is reset (otherwise, ^{41}Ca/^{40}Ca is overabundant by a factor of $\sim 10^2$ compared to ^{26}Al/^{27}Al). Rocks in different parts of the system—deep in the reconnection ring, well inside the x-region, or in a transition zone somewhere in between—have different levels of shielding by nebular gas. The refractory precursors to normal CAIs have negligible shielding from the effects of particle irradiation, while many or most chondrules are fully shielded. The progression from the highest levels to lowest levels of ^{26}Al/^{27}Al would then not represent the effects of radioactive decay before the resolidification of rock melts but rather different levels of original production.

4. In the x-wind picture, rocks that do not undergo extreme heating experience neither particle irradiation nor homogenization. Thus, pristine matrix (not chondrule or CAI fragments) containing unheated, and thus unmixed, presolar grains that are highly isotopically anomalous on a grain-to-grain basis are natural predictions of our model (where the disk in the asteroid belt and beyond is relatively cool, as suggested by arguments that Jupiter formed early beyond the ice-condensation radius). The survival of presolar grains is problematical in scenarios that couple a fast triggering of the formation of the solar system with a hot nebular disk at the position of the asteroid belt.

5. Conventional arguments against cosmic-ray irradiation, such as the overproduction of light element isotopes compared to the meteoritic evidence (Ramaty et al. 1996), lose force in reconnection-ring irradiation models, since the standard target atoms, C, N, and O, for producing Li, Be, or B by spallation reactions are volatile and underrepresented in the precursor rock phases of CAIs or chondrules (Anders & Grevesse 1989). Moreover, any light elements made spallogenically from the O bound up as oxides or silicates in the precursor solids would be largely outgassed in the subsequent heating episodes accompanying launch of CAIs and chondrules in the x-wind. Similarly, since the irradiation occurs before the last annealing of CAIs and chondrules (which can occur even if these objects are only heated and not melted in the x-wind), tell-tale cosmic-ray tracks

[3] Shahijpal et al. (1995) find that ^{41}K*/^{40}Ca is less than 3×10^{-9} in the hibonite inclusion HAL, which has the lowest well-documented ^{26}Al/^{27}Al on record (5×10^{-8}). These authors claim this result as evidence for a correlation between ^{41}Ca and ^{26}Al.

will be erased from the meteoritic record, leaving only nucleosynthetic fossils as clues of the passage of these evanescent particles 4.56×10^9 yr ago.

8. SUMMARY

In this paper, we have reexamined the possibility that short-lived radionuclides might be produced by solar cosmic-ray bombardment of premeteoritic rocks in the early solar system (Fowler et al. 1962; Clayton et al. 1977; Dwek 1978; Lee 1978; Feigelson 1982; Clayton & Jin 1995a, 1995b). Adopting impulsive flares in the reconnection ring of the fluctuating x-wind model (Shu et al. 1997) as the basic irradiation source offers several advantages over previous versions of this idea.

1. Particle irradiation of chondrule and CAI precursors is then a natural by-product of the energetic environment that produces their heating and melting on timescales of hours to days.

2. Irradiation of the relevant rocks occurs in a relatively gas-poor environment and in the region where the cosmic rays are themselves accelerated. Thus, there is a minimal wastage of particles associated with energy losses in the gas (rather than the premeteoritic rock) and with propagation into interplanetary space (rather than onto the target rocks).

3. Conservative scalings from the observed hard X-ray emission in protostars to their flare-generated cosmic-ray ions yield a correct order-of-magnitude acceleration efficiency ϵ_{10} (eq. [7]) to give the required production for any one of the classical short-lived radionuclides ^{26}Al, ^{41}Ca, and ^{53}Mn inferred for the CAIs of chondritic meteorites (see Table 1).

4. Once the absolute scaling ϵ_{10} has been chosen (for given F), the problem in principle has no further adjustable parameters, because (a) the nuclear cross sections are probably known to an accuracy of a factor of a few, (b) the relative abundances of cosmic rays and their energy spectra are known in the modern sun to about 1 significant figure, and (c) the relative abundances of the target atoms in the rock are known to 2 or more significant figures. Thus, there is little freedom left to adjust the relative ratios of ^{26}Al/^{27}Al, ^{41}Ca/^{40}Ca, ^{53}Mn/^{55}Mn, ^{138}La*/^{139}La once we fix one of them. Except for one glaring problem, our model can correctly reproduce the measured ratios of these four quantities in CAIs to within the uncertainties in the cross sections. To obtain the correct generation of ^{26}Al, we must invoke significant ^{3}He reactions, and such reactions correspondingly overproduce ^{41}Ca by 2 orders of magnitude.

5. We see three possible escapes from this conundrum. (a) Thick protoCAI mantles shield the target ^{40}Ca from making ^{41}Ca. This alternative yields the correct ratios for ^{26}Al/^{27}Al, ^{41}Ca/^{40}Ca, ^{53}Mn/^{55}Mn, ^{138}La*/^{139}La using the single mechanism of irradiation of protoCAIs in the reconnection ring, plus it allows a fraction of the CAIs (roughly one-third) to have zero ^{26}Al/^{27}Al because they are launched by the x-wind without having ever entered the irradiation zone. (b) The ^{41}Ca clock is reset by later events. This alternative is natural in models that invoke equilibration of Mg isotope ratios in CAIs instead to explain the bimodal distribution displayed in Figure 1. (c) The irradiation is associated with gradual flares rather than with impulsive flares so that ^{3}He reactions contribute insignificantly. This alternative reproduces the ratios measured for ^{41}Ca/^{40}Ca, ^{53}Mn/^{55}Mn, ^{138}La*/^{139}La in CAIs, but it requires that ^{26}Al be created by some other mechanism, e.g., external seeding.

6. The reconnection-ring model implies that fully irradiated CAIs should have a ^{138}La excess compared to ^{139}La that is 6 times higher than the previously measured bulk value for chondritic meteorites (Shen et al. 1994). This prediction is consistent with the new measurements of Shen et al. (1998), but the expected correlation with the ^{26}Al/^{27}Al value of the CAIs is not observed. We speculate that the lack of correlation may indicate two epochs of irradiation: an earlier stage involving irradiation of CAI precursor rocks by impulsive flares near the protosun, and a later stage involving the effects of gradual flares on the regoliths of bodies in the asteroid belt. To further test the basic irradiation hypothesis, we compute that ^{50}V should have an excess relative to ^{51}V that is 0.3%–0.6% higher in CAIs than the canonical value $^{50}\mathrm{V}/^{51}\mathrm{V} = 2.5 \times 10^{-3}$. We look forward to experimental confrontations of this prediction.

7. The reconnection-ring mechanism fails by 2 or more orders of magnitude to explain the ^{60}Fe abundance that has been inferred for stony meteorites (see Table 1). It may be possible to understand the same data in terms of ^{60}Ni* production by SEP irradiation of the iron in basaltic rocks on Vesta's surface. If, on the other hand, further investigation reveals that ^{60}Fe must have been present in live form in eucrites, then the evidence becomes almost incontrovertible for a late injection event of material by a stellar source rich in free neutrons. If a supernova of Type II is this event and also injected ^{26}Al at the level indicated in Table 1, the differentiation of the parent body of Juvinas and Chervony Kut can be deduced to have occurred $\sim$11 Myr later (Wasserburg, Gallino, & Busso 1998), contrary to the conventional view of a much shorter interval between injection and differentiation (Shukolyukov & Lugmair 1993a, 1993b; Allègre, Manhès, & Göpel 1995; Wasserburg, Busso, & Gallino 1995).

The work of T. L. is supported by R. O. C. National Science Council grants 85-2112-M001-024 and 86-2112-M001-033; that of F. H. S., H. S., and A. E. G., by a NASA grant from the Origins of Solar Systems Program; that of KER by the US Department of Energy, Nuclear Physics Division, under contract no. W-31-109-ENG-38. We thank Al Cameron, Don Clayton, Jitendranath Goswami, Raymond Jeanloz, Guenter Lugmair, Eduardo Martin, Kunihiko Nishiizumi, Jason Shen, and Jerry Wasserburg for illuminating discussions.

APPENDIX A

DIFFICULTIES WITH SYNTHESIS BY GALACTIC COSMIC RAYS

The discovery of unexpectedly high levels of gamma-ray emission at 4.4 and 6.1 MeV from excited nuclei of C and O in the Orion star-forming region has triggered examination of an interesting alternative: cosmic-ray spallation reactions in the interstellar medium. This scheme introduces, however, considerable difficulties.

From the gamma-ray line widths and overall energetics, Bloemen et al. argue that the nuclear excitation of C and O in the Orion molecular cloud occurs by the collision of fast C and O nuclei with the protons in interstellar hydrogen molecules (Bloemen et al. 1994; Bloemen et al. 1997). Adopting this hypothesis, Clayton assumes normal abundances for other heavy cosmic-ray nuclei in comparison with the deduced values of carbon and oxygen (Clayton 1994). He then calculates that the spallation reactions that may be expected when these heavy nuclei interact with interstellar protons will produce $^{26}Al/^{27}Al$, $^{60}Fe/^{56}Fe$, $^{107}Pd/^{108}Pd$, and $^{92}Nb/^{93}Nb$ in roughly their observed proportions, if one chooses the fluence for cosmic-ray exposure to get one of the ratios correctly.

Unfortunately, fitting the observed gamma-ray data in Orion requires cosmic rays that have a concomitant ionization rate per hydrogen atom $\zeta \sim 1 \times 10^{-13}$ s^{-1} (Bloemen et al. 1994; Bloemen et al. 1997; Ramaty et al. 1996). The cosmic-ray bombardment is then too weak by factors of 10–1000 to produce the meteoritic level of $^{26}Al/^{27}Al \sim 5 \times 10^{-5}$. The radionuclide ^{41}Ca can be produced at the requisite rate by this mechanism, but, within the very short period of 1 mean-life (0.15 Myr) of its production, it needs to be incorporated inside meteoroids if it is to account for an abundance level of $^{41}Ca/^{40}Ca \sim 1.5 \times 10^{-8}$ (Ramaty et al. 1996).

A number of other astrophysical considerations suggest that the value $\zeta \sim 1 \times 10^{-13}$ s^{-1} is already too high. Since each ionization deposits on average $\sim 10^{-10}$ ergs of heat into the interstellar medium (Spitzer & Tomasko 1968; Field, Goldsmith, & Habing 1969), the corresponding energy loss in the partial ionization of the roughly 10^{62} H atoms ($\sim 10^5\ M_\odot$ of H_2 gas) in the Orion molecular cloud equals $\sim 10^{39}$ ergs s^{-1}. This dissipation rate in cosmic rays exceeds the entire photon luminosity of all the young stars currently known to reside in the Orion nebula (Cowsik & Friedlander 1995). Moreover, the rate $\zeta \sim 1 \times 10^{-13}$ s^{-1} is about 300 times larger than the values deduced from interstellar chemistry arguments in regions of high-mass star formation elsewhere in the Galaxy that are similar to the Orion molecular cloud (Lepp 1994; Helmich et al. 1995).

In our opinion, these contradictions indicate that the cosmic rays responsible for producing the Orion gamma rays do not roam throughout the clouds of neutral gas in the Orion nebula where most sunlike stars are being born. More likely, they are restricted to the ionized (H II) regions near the birthplaces of high-mass stars, where few constraints exist on the extra ionization produced by cosmic rays above the almost complete levels set by ultraviolet photons. A model of the solar system forming from a photoionizing globule or protoplanetary disk embedded in an ancient H II region may warrant further study.

APPENDIX B

NUCLEOSYNTHESIS OF ^{60}Fe BY PROTOSTELLAR ENERGETIC PARTICLES

Excess ^{60}Ni that correlates with ^{56}Fe has been measured in two stony meteorites, the eucrites (basaltic achondrites) Chervony Kut (Shukolyukov & Lugmair 1993a) and Juvinas (Shukolyukov & Lugmair 1993b). The excess ^{60}Ni is usually interpreted as coming from the beta decay of ^{60}Co, which itself results from the beta decay of ^{60}Fe. In this appendix, we demonstrate why charged-particle irradiation of CAI and chondrule precursors is unlikely to have produced the inferred $^{60}Fe/^{56}Fe$ ratios.

The basic difficulty arises because ^{60}Fe is so neutron rich in comparison with ^{56}Fe, which is the most stable and by far the most abundant species in its region of the chart of nuclides. As a consequence, ^{60}Fe is relatively isolated from neighboring stable nuclei. Reactions involving common targets and projectiles then tend to have small cross sections (unlikely pathways), whereas reactions involving uncommon targets or reactants suffer from small relative abundances.

For example, Clayton & Jin (1995b) proposed the proton and α reactions, $^{64}Ni(p, p\alpha)^{60}Fe$ and $^{58}Fe(\alpha, 2p)^{60}Fe$, which start from the neutron-rich nuclides ^{64}Ni ($\Delta N = 8$) and ^{58}Fe ($\Delta N = 6$). They guessed that the first reaction has a cross section of the order of 50 mbarn, which would make it a modest contributor to the reconnection-ring scheme. Unfortunately, we have carried out Hauser-Feshbach calculations for these reactions and estimate that their cross sections are in the range 50–150 μbarn. We also considered a two-stage variant of the scheme: $^{64}Ni(p, p')^{64}Ni'$ with $^{64}Ni'$ excited to a nuclear level more than 8.1 MeV above ground, followed by the α decay of $^{64}Ni'$ to ^{60}Fe. Again, our calculations imply that the inelastic scattering cross section for the excitation of ^{64}Ni by protons is small; moreover, the decay of the excited $^{64}Ni'$ occurs primarily by the evaporation of neutrons rather than by the emission of an α. Similarly, the reaction $^{58}Fe(\alpha, 2p)^{60}Fe$ has been experimentally measured at 55 MeV, and the total cross section is of order 0.1 mbarn. We have considered many other proton and α reactions, including $^{62}Ni(p, 3p)^{60}Fe$ and $^{59}Co(\alpha, 3p)^{60}Fe$, and we find that their cross sections are all significantly less than 1 mbarn, too small to be important for our purposes.

Of the remaining abundant projectile (in impulsive flares), ^3He suffers from the disadvantage that it is neutron poor; ^3He on any neutron-rich nuclide is likely to *reduce* the neutron excess with (^3He, $p2n$) reactions. Thus, its reactions with common Fe, Ni, or Co isotopes cannot yield much ^{60}Fe. Proton-removing reactions, such as $^{61}Ni(^3He, 4p)^{60}Fe$, have very small cross sections according to our Hauser-Feshbach calculations.

Because light-ion reactions initiated by p, ^3He, and α are ineffective, we examine the potential of heavy-ion reactions. The relevant pairs of reactants are those that are abundant in protostellar flares and in meteorite rock precursors. In impulsive flares, Ne, Mg, Si, and Fe have appreciable relative abundances, in the last three cases enhanced over cosmic values by a factor of 10–20, e.g., Fe/O $\sim$ 1 (Reames 1996). In the target solids, O, Mg, Si, and Fe are generally important and, in CAIs, Ca, Al, and Ti are prospective reactants. Although we consider reactions with substantial threshold energies, $\sim$10 MeV, they are small compared to the energy available in heavy-ion reactions,

$$E_a = \left(\frac{A_2}{A_1 + A_2}\right) E_1 , \tag{B1}$$

where subscripts 1 and 2 refer to the beam and solid particle, respectively. When the beam energy per nucleon, E_1/A_1, exceeds 1 MeV amu^{-1}, the beam particle brings in sufficient energy to exceed the thresholds. The Coulomb barrier has a greater potential for influencing heavy-ion reactions. For nuclide pairs in the range from O to Ni, however, there is sufficient energy to overcome the Coulomb barrier in all cases once $E_1/A_1 > 3$ MeV amu^{-1}.

Aside from inelastic scattering, the first important type of heavy-ion reaction to consider is neutron transfer, which can occur well below the Coulomb barrier. For relevant projectiles on Fe, this barrier is around $E_1/A_1 = 2$ MeV amu^{-1}. Neutron transfer reactions have been studied in great detail, and they have been reviewed by Rehm (1991) and van Oertzen (1990). The cross section for the transfer of a single neutron can reach several hundred millibarns when the reaction energy approaches the Coulomb barrier. However, this occurs only if the reaction energy (or Q-value) is positive or is negative by only a few MeV (see, e.g., Fig. 16 of Rehm 1991). To synthesize ^{60}Fe, we consider the transfer of 2, 3, and 4 neutrons to ^{58}Fe, ^{57}Fe. and ^{56}Fe, respectively. The transfer of each additional neutron is progressively more difficult, e.g., the cross section for an M-neutron transfer is reduced by approximately 4^{M-1} below that for a 1 neutron transfer (cf. Fig. 18 of Rehm 1991; Jiang et al. 1994).

We consider the neutron-transfer cross sections for important neutron-rich projectiles interacting with the three relevant Fe isotopes, ^{56}Fe, ^{57}Fe, and ^{58}Fe (including Fe-Fe reactions, using § 4.2 of Rehm 1991). All three iron isotopes can potentially contribute because their abundances increase with decreasing neutron excess. Unfortunately, very few of the possible reactions have Q-values in the range to give reasonable cross sections. Among those with favorable Q-values, we find the following, in rank order, to be the most important: (1) ^{56}Fe + ^{57}Fe or ^{58}Fe, (2) ^{22}Ne + ^{58}Fe, (3) ^{18}O + ^{56}Fe, ^{57}Fe, and ^{58}Fe, (4) ^{26}Mg + ^{58}Fe. Although these reactions have cross sections in the range 10–200 mbarn, the ^{60}Fe/^{56}Fe ratios produced according to equation (20) are all 3–4 orders of magnitude too small, largely as the result of low abundance factors but also because of the unfavorable factor A/Z^2.

Fusion reactions are the last type of reaction that occurs as the energy approaches and exceeds the Coulomb barrier. When the compound nucleus is formed, the probabilities for the various decay modes are well described by statistical considerations and quantitatively expressed by Hauser-Feshbach calculations. For the relevant energy, $E_1/A_1 \approx 1$–10 MeV amu^{-1}, the fusion reactions of interest involve moderately light energetic particles, such as O and Ne, incident on the nuclei of the heavier, refractory elements found in CAIs, like Ca and Ti. Since ^{60}Fe is quite neutron rich ($\Delta N = 8$), ^{48}Ca ($\Delta N = 8$) and ^{50}Ti ($\Delta N = 6$) are of particular interest. We estimate the cross sections for the formation of ^{60}Fe following the fusion of both ^{16}O and ^{18}O with ^{48}Ca, modeling the decay of the fused nucleus with a Hauser-Feshbach code. In the former case, the cross section reaches 0.4 mbarn at 45 MeV, whereas the cross section for ^{18}O + ^{48}Ca peaks at 56 mbarn at 55 MeV. This large difference between the production cross sections for ^{16}O and ^{18}O on ^{48}Ca underscores the importance of starting with neutron-rich reactants in synthesizing ^{60}Fe. Unfortunately, the low relative abundances of ^{18}O and ^{48}Ca imply that the production of ^{60}Fe by these reactants fall short by several orders of magnitude of the measured value. We found no other fusion reaction pathway to produce ^{60}Fe with a cross section larger than 1 mbarn.

REFERENCES

Allègre, C. J., Manhès, G., & Göpel, C. 1995, Geochim. Cosmochim. Acta, 59, 1445
Anders, E., & Ebihara, M. 1982, Geochim. Cosmochim. Acta, 46, 2363
Anders, E., & Grevesse, E. 1989, Geochim. Cosmochim. Acta, 53, 197
Anders, E., & Zinner, E. 1993, Meteoritics, 28, 490
Bertout, C. 1989, ARA&A, 27, 351
Birck, J.-L., & Allégre, C. J. 1985, Geophys. Res. Lett., 12, 745
Birck, J. L., & Lugmair, G. W. 1988, Earth Planet. Sci. Lett., 90, 131
Blann, M. 1966, Nucl. Phys., 80, 223
Bloemen, H., et al. 1994, A&A, 281, L5
———. 1997, ApJ, 475, L25
Caffee, M. W., Hohenberg, C. M., Swindle, T. D., & Goswami, J.N. 1987, ApJ, 313, L31
Caffee, M. W., et al. 1991, in The Sun in Time, ed. C. P. Sonett, M. S. Giampapa, & M. S. Matthews (Tucson: Univ. Arizona Press), 413
Caillet, C., MacPherson, G. J., & Zinner, E. K. 1993, Geochim. Cosmochim. Acta, 57, 4725
Cameron, A. G. W. 1988, ARA&A, 26, 441
———. 1993, in Protostars and Planets III, ed. E. H. Levy & J. I. Lunine (Tucson: Univ. Arizona Press), 47
———. 1995, Meteoritics, 30, 133
Cameron, A. G. W., Hoflich, P., Myers, P. C., & Clayton, D. D. 1995, ApJ, 447, L57
Carkner, L., Feigelson, E., Koyama, K., Montmerle, T., & Reid, I. N. 1996, ApJ, 464, 286
Clayton, D. D. 1975, Nature, 257, 36
———. 1983, ApJ, 268, 381
———. 1994, Nature, 368, 222
Clayton, D. D., Dwek, E., & Woosley, S. E. 1977, ApJ, 214, 300
Clayton, D. D., & Leising, M. D. 1984, in AIP Conf. Proc. 304, The Second Compton Symposium, ed. C. E. Fichtel, N. Gehrels, & J. P. Norris (New York: AIP), 137
Clayton, D. D., & Jin, L. 1995a, ApJ, 451, L87
———. 1995b, ApJ, 451, 681
Clayton, R. N., Hinton, R. W., & Davis, A. M. 1988, Phil. Trans. R. Soc. London A, 325, 483
Clayton, R. N., & Mayeda, T. K. 1977, Geophys. Res. Lett., 4, 295
Cliver, E. W. 1996, in AIP Conf. Proc. 374, High-Energy Solar Physics, ed. R. Ramaty, N. Mandzhavidze, & X.-M. Hua (New York: AIP), 45
Cowsik, R., & Friedlander, M. W. 1995, ApJ, 444, L29
Cuzzi, J. N., Dobrovolskis, A. R., & Champney, J. M. 1993, Icarus, 106, 102
Diehl, R., et al. 1994, ApJS, 92, 429
———. 1995, A&A, 298, 445
Dwek, E. 1978, ApJ, 221, 1026
Edwards, S., et al. 1993, AJ, 106, 372
Feigelson, E. D. 1982, Icarus, 51, 155
Feigelson, E. D., Jackson, J. M., Mathieu, R. D., Myers, P. C., & Walter, F. M. 1987, AJ, 94, 1251
Field, G. B., Goldsmith, D. W., & Habing, H. J. 1969, ApJ, 155, L149
Fisk, L. 1978, ApJ, 224, 1048
Fowler, W., et al. 1962, JRAS, 6, 148
Frantsvog, D. J., Kunselman, A. R., Wilson, R. L., Zaidins, C. S., & Détraz, C. 1982, Phys. Rev. C, 25, 770
Gavron, A. 1980, Phys. Rev. C, 21, 230
Gensho, R., Nitoh, O., Makino, T., & Honda, M. 1979, Phys. Chem. Earth, 11, 11
Ghosh, P., & Lamb, F. K. 1978, ApJ, 223, L83
Gosling, J. T. 1993, J. Geophys. Res., 98, 4529
Goswami, J. N., Marhas, K. K., & Sahijpal, S. 1996, Meteoritics Planet. Sci. Suppl., 31(4), A52
Grossman, L. 1980, Ann. Rev. Earth Planet. Sci., 8, 559
Haisch, S., Antunes, A., & Schmitt, J. H. M. M. 1995, Science, 268, 1327
Harper, C. L. 1996, ApJ, 466, 1026
Hartmann, L., Cassen, P., & Kenyon, S. J. 1997, ApJ, 475, 770
Hayashi, C., Nakazawa, K., & Nakagawa, Y. 1985, in Protostars and Planets II, ed. D. C. Black & M. S. Matthews (Tucson: Univ. Arizona Press), 1100
Helmich, F. P., et al. 1995, in Physics and Chemistry of Interstellar Molecular Clouds, Proc. 2nd Cologne-Zermatt Symposium, ed. G. Winnewisser & G. C. Pelz (Berlin: Springer), 254
Hutcheon, I. D., Huss, G. R., & Wasserburg, G. J. 1994, Lunar Planet. Sci., 25, 587
Hutcheon, I. D., & Jones, R. H. 1995, Lunar Planet. Sci., 26, 647
Ireland, T. R., Zinner, E. K., Fahey, A. J., & Esat, T. M. 1992, Geochim. Cosmochim. Acta, 56, 2503
Jajina, J., Myers, P.C., & Adams, F. C. 1998, in preparation
Jeffreys, P. M., & Reynolds, J. H. 1961, J. Geophys. Res., 66, 3582
Jiang, C. L., et al. 1994, Phys. Lett. B, 337, 59
Kamata, Y., Koyama, K., Tsuboi, Y., & Yaumuchi, S. 1997, PASJ, 48, 461
Kastner, J. H., & Myers, P. C. 1994, ApJ, 421, 605

Kelly, W. R., & Wasserburg, G. J. 1978, Geophys. Res. Lett., 5, 1079
Königl, A. 1991, ApJ, 370, L39
Koyama, K., Ueno, S., Kobayashi, N., & Feigelson, E. D. 1996, PASJ, 48, L87
LaTourette, T., & Wasserburg, G. J. 1998, Earth Planet. Sci. Lett., submitted
Lau, K. H., Mewaldt, R. A., & Stone, E. C. 1985, Proc. 19th Int. Cosmic Ray Conf. (La Jolla), NASA CP-2376, 3, 91
Lee, D.-C., & Halliday, A. N. 1995, Nature, 378, 771
Lee, T. 1978, ApJ, 224, 217
Lee, T., Papanastassiou, D. A., & Wasserburg, G. J. 1976, Geophys. Res. Lett., 3, 109
———. 1977, ApJ, 211, L107
Lepp, S. 1994, in Astrochemistry of Cosmic Phenomena, ed. P. Singh (Dordrecht: Reidel), 471
MacPherson, G. J., & Davis, A. M. 1993, Geochim. Cosmochim. Acta, 57, 231
MacPherson, G. J., Davis, A. M., & Zinner, E. K. 1995, Meteoritics, 30, 365
Magazzu, A., Martin, E. L., Sterzik, M. F., Neuhäuser, R., Covino, E., & Alcala, J. M. 1997, A&A, 124, 449
Mahoney, W. A., Ling, J. C., Wheaton, W. A., & Jacobsen, A. S. 1984, ApJ, 286, 578
Martin, E. L. 1997, A&A, 321, 492
———. 1998, AJ, 115, 351
McCulloch, M. T., & Wasserburg, G. J. 1978, ApJ, 220, L15
Najita, J. R., & Shu, F. H. 1994, ApJ, 429, 808
Neuhäuser, R. 1997, Science, 276, 1363
Neuhäuser, R., & Preibisch, Th. 1997, A&A, 322, L37
Ostriker, E., & Shu, F. H. 1995, ApJ, 447, 813
Podosek, F. A., et al. 1991, Geochim. Cosmochim. Acta, 55, 1083
Preibisch, Th. 1997, A&A, 324, 690
Ramaty, R., Kozlovsky, B., & Lingenfelter, R. E. 1996, ApJ, 456, 525
Ramaty, R., & Simnett, G. M. 1991, in The Sun in Time, ed. C. P. Sonett, M. S. Giampapa, & M. S. Matthews (Tucson: Univ. Arizona Press), 232
Randich, S. 1998, in Cool Stars in Clusters and Associations, ed. G. Micela, R. Pallavicini, & G. Sciortino (Rome: Mem. Soc. Astron. Italiana), in press
Reames, D. V. 1995, Rev. Geophys. Suppl., 33, 585
———. 1996, in AIP Conf. Proc. 374, High-Energy Solar Physics, ed. R. Ramaty, N. Mandzhavidze, & X. Hua (New York: AIP), 35
Reames, D. V., Barbier, L. M., Von Rosenvinge, T. T., Mason, G. M., Mazur, J. E., & Dwyer, J. R. 1997, ApJ, 483, 515
Reedy, R. C., & Marti, K. 1991, in The Sun in Time, ed. C. P. Sonett, M. S. Giampapa, & M. S. Matthews (Tucson: Univ. Arizona Press), 260
Rehm, K. E. 1991, Annu. Rev. Nucl. Part. Sci., 41, 429
Reynolds, J. H. 1960, Phys. Rev. Lett., 4, 8
Russell, S. S., Srinivasan, G., Huss, G. R., Wasserburg, G. J., & MacPherson, G. J. 1996, Science, 273, 757
Sahijpal, S., Srinivasan, G., Wasserburg, G. J., & Goswami, J. N. 1995, Meteor. Planet. Sci., 30, 570
Schopper, C. H. 1991, Landolt-Bornstein, Vol. 13 (Berlin: Springer)
Shen, J. J. S., Ho, C. J., & Lee, T. 1998, Science, submitted
Shen, J. J. S., Lee, T., & Chang, C. T. 1994, Geochim. Cosmochim. Acta, 58, 1499
Shu, F. H., Adams, F. C., & Lizano, S. 1987, ARA&A, 25, 23
Shu, F. H., Shang, H., Glassgold, A. E., & Lee, T. 1997, Science, 277, 1475
Shu, F. H., Shang, H., & Lee, T. 1996, Science, 271, 1545
Shukolyukov, A., & Lugmair, G. W. 1993a, Science, 259, 1138
———. 1993b, Earth Planet. Sci. Lett., 119, 159
Spitzer, L., & Tomasko, M. G. 1968, ApJ, 152, 971
Srinivasan, G., Sahijpal, S., Ulyanov, A. A., & Goswami, J. N. 1996, Geochim. Cosmochim. Acta, 60, 1823
Srinivasan, G., Ulyanov, A. A., & Goswami, J. N. 1994, ApJ, 431, L67
Swindle, T. D. 1993, in Protostars and Planets III, ed. E. H. Levy & J. I. Lunine (Tucson: Univ. Arizona Press), 867
Temerin, M., & Roth, I. 1992, ApJ, 391, L105
Van Hollebeke, M. A. I., Sung, M., & McDonald, F. B. 1975, Sol. Phys., 41, 189
van Oertzen, W. 1990, Inst. Phys. Conf. Ser., 109, 71
Warren, P. 1991, J. Geophys. Res., 96(B4), 5909
Wasserburg, G. J. 1985, in Protostars and Planets II, ed. D. C. Black & M. S. Matthews (Tucson: Univ. Arizona Press), 703
Wasserburg, G. J., Busso, M., & Gallino, R. 1995, ApJ, 440, L101
———. 1996, ApJ, 466, L109
Wasserburg, G. J., Busso, M., Gallino, R., & Raiteri, C. M. 1994, ApJ, 424, 412
Wasserburg, G. J., Gallino, R., & Busso, M. 1998, ApJ, 500, L189
Wasserburg, G. J., Lee, T., & Papanastassiou, D. A. 1977, Geophys. Res. Lett., 4, 299
Weidenschilling, S. J. 1977, Icarus, 180, 57
Whipple, F. L. 1972, in From Plasma to Planet, ed. A. Elvius (New York: Wiley), 211
Wood, J. A. 1996, in Chondrules and the Protoplanetary Disk, ed. R. H. Hewins, R. H. Jones, & E. R. D. Scott (New York: Cambridge Univ. Press), 55
Wooden, J. L., Nyquist, L. E., Bogard, D. D., Shih, C. Y., Bansai, B. M., Wiesman, H., & McKay, G. A. 1979, LPSC X, 1379